Coupled chemo-mechanical deterioration of cementitious materials. Part I: Modeling

Detlef Kuhl [*], Falko Bangert, Günther Meschke

Institute for Structural Mechanics, Ruhr University Bochum, Universitätsstr. 150 IA6-28, 44780 Bochum, Germany

Abstract

The paper is concerned with a coupled chemo-mechanical model describing the interaction of calcium leaching and mechanical damage in cementitious materials on a macroscopic level. Starting from the definition of the total porosity described in terms of the chemical dissolution and mechanical damage and the assumptions of chemical and mechanical potentials, the model is consistently developed within the theories of mixtures and thermodynamics. The displacement vector and the calcium concentration of the pore fluid are taken as the primary variables of the coupled field problem. The model is able to capture degradation of the stiffness and strength following from chemical and mechanical damage as well as the increasing conductivity due to matrix dissolution and the opening of micro-cracks. The irreversible character of chemical and mechanical degradation processes is taken into account by internal variables and related chemical reaction and mechanical damage criteria together with conditions for progressing chemical dissolution in the form of Kuhn–Tucker conditions. The properties and the capabilities of the present model are illustrated by a detailed analysis.
© 2003 Published by Elsevier Ltd.

1. Introduction

The durability of concrete structures is considerably affected by the accumulation of damage resulting from time variant external loading in conjunction with environmentally induced mechanisms such as moisture and heat transport, freeze-thaw actions, chemically expansive reactions, chemical dissolution or by the corrosion of the reinforcement. Out of the wide range of environmentally induced deterioration mechanisms the coupled effects calcium leaching and mechanical damage in structures made of cementitious materials such as concrete exposed to aggressive environmental conditions are addressed in the present paper.

---

[*] Corresponding author. Tel.: +49-234-322-9055; fax: +49-234-321-4149.

E-mail addresses: detlef.kuhl@ruhr-uni-bochum.de (D. Kuhl), falko.bangert@ruhr-uni-bochum.de (F. Bangert), guenther. meschke@ruhr-uni-bochum.de (G. Meschke).

Long-term degradation of concrete structures under permanently aqueous environmental conditions is mainly controlled by interacting chemical and mechanical processes leading to the destruction of the micro-structure of the material resulting from the dissolution of soluble cement constituents such as calcium hydroxide, calcium silicate hydrate (CSH) and ettringite and the opening and propagation of micro-cracks. Ultimately, collapse of concrete structures may be caused by the superposition of both deterioration mechanisms, even if the individual degradation processes are not critical for the structural integrity. Considerable progress has been archived in material oriented research to obtain a better insight into the individual transport processes and mechanical and chemical damage mechanisms, respectively. As far as computational modeling of coupled mechanical and dissolution-induced degradation on a macroscopic level is concerned, recent progress in durability mechanics (see e.g. Coussy et al., 1999; Coussy and Ulm, 2001), together with adequate numerical methods, opens the perspective of bridging the gap between research on the material and on the structural level.

1.1. Chemical and chemo-mechanical deterioration of concrete: experimental evidence

The contact of hardened cement paste with water, as a special case of an aggressive environmental media, leads to the diffusion of calcium ions associated with concentration gradients between the interstitial water and the aggressive solvent outside the cement sample. As a consequence of the disturbed chemical equilibrium state, chemical reactions between the cementitious skeleton and the pore fluid occur. The leaching of a pure cement paste in contact with deionized water leads to a total dissolution of portlandite and ettringite and to a progressive decalcification of CSH-phases. This dissolution mechanism results from the chemical imbalance between the bounded cement constituents and the pore solution which is controlled by the diffusion of calcium ions from the interstitial solution of the cement paste to the aggressive solvent (water) resulting from the chemical imbalance between both fluids. As a consequence of the decalcification of the cement paste the mechanical as well as the transport properties of cementitious materials are changed.

In the pioneering experiments by Berner (1988, 1992) on the dissociation of cement paste the strong influence of chemistry on the long-term behavior of cementitious materials are investigated. The experimental data give evidence for the dependence of the decalcification of cement constituents on the calcium ion concentration of the pore fluid. In the experimental work performed by Adenot (1992) and Adenot and Buil (1992) it is shown, that the pore solution is in a local chemical equilibrium with the solid phase. In the solid phase of the specimens an uncorroded core and different corroded zones separated by dissolution fronts are observed. The inner front is associated with the dissolution of calcium hydroxide (portlandite) and the outer fronts are associated with progressive decalcification of the CSH-phases. Based on Berner's experimental data, Gérard (1996, 2000) and Delagrave et al. (1997) propose an empirical function $s(c)$ relating the calcium concentration of the pore fluid c to the calcium concentration of the cementitious skeleton s for instantaneous dissolution processes, i.e. assuming chemical equilibrium between the solid and fluid phase. Delagrave et al. (1997) have observed, that the calcium content of a cement sample is primarily reduced in two steps, which can be identified as the dissolution fronts of portlandite and CSH-phases.

Since the calcium leaching kinetics in water is very slow, the majority of experiments on calcium leaching of cement samples are performed by accelerated test methods using strongly concentrated ammonium nitrate solutions instead of deionized water (Carde et al., 1996, 1997a,b; Carde and François, 1997; Heukamp et al., 2001a; Ulm et al., 2001). The equivalence of the leaching process in samples exposed to deionized water and to ammonium nitrate solution is shown by Carde et al. (1997a) by means of chemical analyses of standard and accelerated leached cement samples. Only the dissolution of ettringite is not captured by this accelerated test method. According to Carde et al. (1997a), however, this mineral has only a marginal influence on the mechanical properties. To the best knowledge of the authors, the only real life time experiment documented in the open literature has been performed by Trägårdh and Lagerblad (1998).

They investigated a concrete sample subjected to deionized water from a water reservoir for 90 years. In accordance with Carde et al. (1996, 1997a,b) and Carde and François (1997), they observed an increased porosity resulting from the dissolution of cement phases within a degradation zone of approximately 9 mm thickness separated from the sound material by the dissolution front of portlandite crystals.

The influence of calcium leaching on the mechanical properties and the porosity of cement paste is investigated on micro-cylinder cement paste samples subjected after accelerated leaching to uniaxial compression and water porosity tests (Carde et al., 1996, 1997a,b; Carde and François, 1997), respectively. The total leaching of portlandite and the progressive decalcification of CSH-phases leads to a linear dependence of the porosity and the strength on the ratio between the degraded and the sound cross-sections. Compared to the virgin material the ductility of the chemically degraded material is larger because the micro-structure of the material is modified by leaching. Furthermore, stress–strain diagrams given by Carde and François (1997) and Carde et al. (1996) illustrate, that the stiffness of the material is significantly reduced due to calcium leaching. From triaxial tests of cylindrical cement samples subjected to accelerated leaching (Heukamp et al., 2001a; Ulm et al., 2001) a strong dependence of the mechanical properties on the pore pressure due to the increased pore space and the reduction of the materials frictional performance of the leached cement paste is found.

The calcium ion transport through the pore space is investigated by Delagrave et al. (1997) and Adenot (1992). It is found, that the conductivity depends non-linearly on the porosity and the calcium concentration of the pore solution and that the conductivity significantly increases with propagating chemical degradation. An interesting aspect concerning a comparison between experimentally and numerically obtained propagation of the portlandite dissolution front is addressed in Delagrave et al. (1997). According to this work, the numerical analysis is only able to fit the experiments, if only 50% of the conductivity of the pore fluid with respect to calcium ions in pure water is taken. This indicates, that the calcium ion conductivity of the pore fluid increases as the calcium concentration c decreases with propagating chemical dissolution.

First experiments concerning coupled chemo-mechanical degradation on the structural level are performed by Le Bellégo et al. (2000, 2001a,b, 2003). The influence of chemical degradation on the mechanical structural behavior is investigated by means of mortar beams exposed to ammonium nitrate solution on the front and back face, introducing unidirectional leaching fronts moving through the thickness of the beam. At different stages of the chemical attack the beam is subjected to a vertical load up to ultimate failure. Depending on the immersion time of calcium leaching the decrease of the stiffness, the strength, the fracture energy and, consequently, the internal length is recorded. Recently, Le Bellégo et al. (2001b) proposed an alternative three-point bending test, where simultaneously to the mechanical load a part of the bottom surface of the beam is exposed to an aggressive ammonium nitrate solution. After increasing the displacement controlled loading, the displacement is held constant. In this phase of the test the reaction force is reduced due to calcium leaching. Subsequently to this coupled chemo-mechanical experiment a standard mechanical loading test up to the ultimate failure is carried out. The results are compared to respective results from a mortar beam subjected in the first phase of the experiment only to chemical attack. The resulting load–displacement diagrams clearly demonstrate that the reduction of the stiffness and strength is significantly larger in the coupled chemo-mechanical experiments. This indicates, that micro- and macro-cracking increases the conductivity and, consequently, accelerates the chemical degradation.

1.2. Chemical and chemo-mechanical deterioration of concrete: material modeling

Based on the experimental results on calcium leaching and coupled chemo-mechanical damage, material models formulated on a macroscopic level of observation, have been developed for numerical predictions of the life time of concrete structures. One type of models is based on the pioneering work by Gérard (1996) and subsequent publications (Gérard, 2000; Gérard et al., 1998; Pijaudier-Cabot et al., 1998a,b, 2002; Le

Bellégo et al., 2000, 2001a,b). It is based on a phenomenological chemical equilibrium model relating the calcium concentration of the skeleton and the pore solution $s(c)$ and on the concept of isotropic damage mechanics. From the calcium content of the skeleton, the porosity, the aging variable accounting for the increase of the mechanical properties due to calcium leaching and the conductivity are determined by several empirical models. The influence of mechanical damage on the calcium ion conductivity is also considered by an empirical model. This model is able to capture the main characteristics of coupled chemo-mechanical damage described above. However, only the maximum diffusivity of calcium ion transport associated either with mechanically induced damage or with chemical deterioration of concrete is considered. Ulm et al. (1999, 2001) propose a chemo-plasticity model formulated within the theory of porous media (Coussy, 1995). This model is also based on a chemical equilibrium model, using empirical relations for the conductivity and aging. In both models, the irreversible character of skeleton dissolution is not accounted for. Hence, chemical unloading or cyclic chemical loading processes cannot be described.

From the experimental results, the key-role of the porosity for the changing material and transport properties of chemo-mechanically loaded cementitious materials becomes obvious. Based on this observation a fully coupled chemo-mechanical damage model is developed within the framework of the theory of mixtures (Bowen, 1976) in this paper. The material is described as ideal mixture of the fully saturated pore space and the matrix. In this model, the pore fluid acts as a transport medium for calcium ions. The pore pressure, however, is not accounted for in the present version of the model. Based on first ideas by Kuhl et al. (2000) the changing mechanical and transport properties are related to the total porosity defined as the sum of the initial porosity, the chemically induced porosity and the apparent mechanical porosity. Together with the assumptions of chemical and mechanical potentials the need for further assumptions or empirical models is circumvented. Micro-cracks are interpreted according to Kachanov (1958) as equivalent pores affecting, on a macroscopic level, the conductivity and stiffness but not the mass balance. The dissolution of calcium of the cementitious skeleton is interpreted as an enlargement of the pores affecting the mass balance and the mechanical as well as the transport properties of the material. The phenomenological chemistry model proposed by Gérard (1996) is used to describe the chemical equilibrium between the solid and liquid phase and to calculate the chemically induced porosity. To account for the irreversible character of the skeleton dissolution a chemical reaction criterion and a related internal variable are introduced in analogy to a mechanical damage criterion (see e.g. Simo and Ju, 1987). The constitutive laws for the chemical and mechanical sub-problem are consistently derived within the framework of thermodynamics. Apart from the constitutive laws also criteria for propagating matrix dissolution (chemical loading/unloading criteria) are obtained without any additional assumptions. Analogous criteria have been obtained previously from an analysis of the chemical system by Mainguy and Coussy (2000). The concentration dependence of the calcium ion conductivity of the pore fluid on the calcium concentration is considered by using the theory of strong electrolytes. This approach allows the determination of the two diffusion constants similar to Kohlrausch's (1900) and Kohlrausch and von Steinwehr's (1902) empirical molar conduction model. From ion–ion interactions in the pore fluid, the model yields a reduction of the conductivity of pure water proportional to the square root of the calcium ion concentration.

1.3. Outline of the paper

Section 2 is concerned with the development of a coupled chemo-mechanical damage model based upon the mass balance of calcium ions, the balance of momentum and related constitutive laws and with comparisons with other existing models and experimental results, respectively. Studies on the material point level in Section 3 illustrate the characteristics of matrix dissolution and coupled chemo-mechanical deterioration of cementitious materials. Numerical methods for the solution of the coupled non-linear initial boundary value problem of calcium leaching and mechanically induced damage as well as representative applications to concrete structures are contained in the second part of the paper (Kuhl et al., in press).

2. Modeling of coupled chemo-mechanical damage

As described in the introduction experimental evidence shows, that the change of the mechanical properties of cementitious materials is related to the additional porosity resulting from the dissolution of cement constituents. Due to the increasing pore space the transport conditions for dissolved constituents within the pore fluid are improved. On the other hand, the volume fraction of the cementitious skeleton is reduced and, consequently, the stiffness and strength are reduced. With the chemo-mechanical damage model developed in this paper the mechanical consequences of chemical matrix dissolution and mechanically induced damage can be captured in a consistent manner by the theory of mixtures (Bowen, 1976). According to this macroscopic theory, the pore space and the skeleton are responsible for the transport and the mechanical properties of the macroscopic material, respectively. Within this framework, the volume fraction of the skeleton material is reduced by the dissolution of cement constituents (chemically induced pore space) as well as by mechanical damage (mechanically induced apparent pore space).

2.1. Phenomenological description of chemo-mechanical damage

The main characteristic's of chemo-mechanical damage can be explained, if cementitious materials are considered as porous materials consisting of the connected pore space and the cementitious skeleton (compare Fig. 1). In the chemically sound cement paste the solid constituents contained in the cementitious skeleton and the substances constituting the pore fluid (cations, anions and water) are in a state of chemical equilibrium. If the environmental conditions are changed by exposing the structure to deionized water at the surface, the resulting concentration gradient between the pore fluid and the deionized water leads to the migration of anions, cations and other dissolved substances towards the surface of the cementitious structure. Consequently, the ion concentration in the pore fluid is reduced and the chemical equilibrium is violated. To restore chemical equilibrium, more substances of the skeleton are dissolved instantaneously. In particular, calcium hydroxide (portlandite), ettringite and CSH-phases are dissociated at different states of the cement dissolution process (see e.g. Adenot, 1992; Adenot and Buil, 1992; Berner, 1988, 1992; Gérard, 1996, 2000). The main chemical reactions are the dissociation of portlandite,
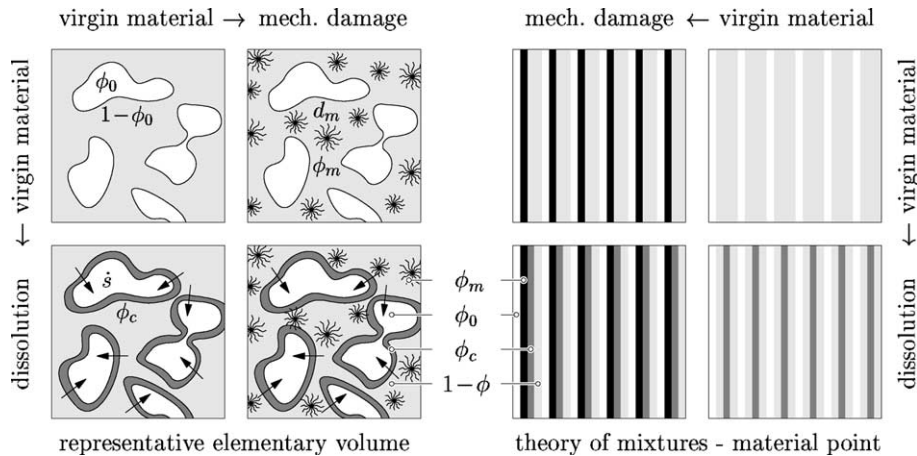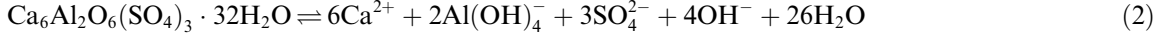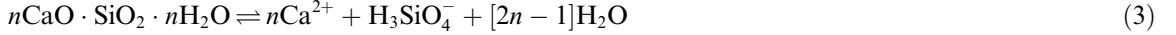
$$Ca(OH)_2 \rightleftharpoons Ca^{2+} + 2OH^- \tag{1}$$

Fig. 1. Chemo-mechanical damage of porous materials within the theory of mixtures.

ettringite

$$Ca_6Al_2O_6(SO_4)_3 \cdot 32H_2O \rightleftharpoons 6Ca^{2+} + 2Al(OH)_4^- + 3SO_4^{2-} + 4OH^- + 26H_2O \tag{2}$$

and a number of distinct forms of CSH:

$$nCaO \cdot SiO_2 \cdot nH_2O \rightleftharpoons nCa^{2+} + H_3SiO_4^- + [2n-1]H_2O \tag{3}$$

Dissociation results in double charged calcium cations, different anions (OH^-, $Al(OH)_4^-$, SO_4^{2-}, $H_3SiO_4^-$) and water (H_2O), constituting a strong electrolyte solution. The dissolution process can be interpreted as micro-diffusion, where the size of the pores being increased by the dissolution of the surrounding cement substances (see Fig. 1). As a result of the increasing pore space, the transport of the reaction products is improved and the mechanical performance of the skeleton is weakened. Eqs. (1)–(3) indicate the relevance of the amount of calcium ions within the pore space with regards to the state of chemical equilibrium. According to Berner (1988, 1992) the calcium cation concentration in the pore fluid can be used as a primary variable to describe the dissolution–diffusion process of calcium leaching. At higher concentrations calcium hydroxide is dissolved first. With decreasing concentrations, ettringite and CSH are dissolved. In summary, the gradient of the calcium ion concentration governs the transport of dissolved substances within the fluid-filled pore space and the calcium ion concentration governs the state of chemical degradation of the cementitious skeleton.

External loading leads to the opening and propagation of micro-cracks in cementitious skeleton, and, consequently to a reduction of the stiffness and strength of the macroscopic material and to the increase of the conductivity of reaction products within the pore fluid. If mechanical damage is interpreted as the generation of mirco-pores within the skeleton (see Fig. 1), chemically and mechanically induced damage are mainly coupled by the porosity defined in terms of the initial porosity, the dissolved pore space and the mechanically induced apparent pore space.

2.2. Definition of the total porosity

The total porosity ϕ is defined as the sum of the initial porosity related to the virgin material ϕ_0, the chemical porosity ϕ_c resulting from the skeleton dissolution and the apparent mechanical porosity ϕ_m due to the opening of micro-cracks (compare Fig. 1):

$$\phi = \phi_0 + \phi_c + \phi_m \tag{4}$$

It should be noted, that the apparent porosity affects only the transport, stiffness and strength of the material, but not the mass balance. This assumption is consistent with the fact, that the opening of cracks is not associated with a loss of mass. Both variable porosities ϕ_c and ϕ_m are related to internal variables κ_c and κ_m, which will be described in Section 2.4. The chemical porosity ϕ_c depends on the calcium concentration s of the skeleton material, which in turn depends on the internal parameter κ_c.

$$\phi_c = \phi_c(s(\kappa_c)) \tag{5}$$

The apparent mechanical porosity ϕ_m is obtained by multiplying the scalar damage parameter d_m by the volume fraction of the skeleton $1 - \phi_0 - \phi_c$. This definition of ϕ_m takes into account, that micro-cracking only occurs within the skeleton material. The micro-cracks situated in the cementitious skeleton can be interpreted according to Kachanov (1958) as micro-pores:

$$\phi_m = \phi_m(\phi_c(s(\kappa_c)), d_m(\kappa_m)) = [1 - \phi_0 - \phi_c(s(\kappa_c))]d_m(\kappa_m) \tag{6}$$

A detailed description of the functions $\phi_c(s(\kappa_c))$ and $d_m(\kappa_m)$ and their dependence on the internal parameters and primary variables is given in Sections 2.4.3 and 2.4.5. Based on Eqs. (4) and (6) the apparent volume fractions of the pore space and the skeleton can be formulated as follows:

$$\phi = [\phi_0 + \phi_c][1 - d_m] + d_m, \qquad 1 - \phi = [1 - \phi_0 - \phi_c][1 - d_m] \tag{7}$$

The pore space, corresponding to the sum of all voids within the material, is defined by the sum of the initial porosity ϕ_0 and the porosity ϕ_c created by matrix dissolution. Consequently, the volume fractions of the fluid and the solid phase are given as follows:

$$\phi_0 + \phi_c = \phi - \phi_m, \qquad 1 - \phi_0 - \phi_c = 1 - \phi + \phi_m \tag{8}$$

2.3. Initial boundary value problem

The coupled mechanism of calcium leaching and mechanical damage in porous cement pastes is characterized by the concentration field of calcium ions $c(X)$ and the displacement field $u(X)$ as primary variables as well as by internal variables accounting for the irreversible character of both deterioration processes. The primary variables within the domain Ω are governed by the conservation of the calcium ion mass contained in the pore space and by the balance of linear momentum. This system of differential equations is accompanied by related boundary and initial conditions on the boundary Γ and within the domain Ω.

The molar form of the mass balance of calcium ions contained in the fluid-filled pore space consists of three terms: The spatial change of the mass flux $\operatorname{div} q$, the rate of the calcium ion mass due to the temporal change of the pore space $[\phi_0 + \phi_c]^{\cdot} c$ and the calcium concentration $[\phi_0 + \phi_c]\dot{c}$, defined by the term $[\phi_0 + \phi_c]c]^{\cdot}$, and the calcium mass production $\dot{s}$ due to the dissociation of cement constituents. If volume forces and the linear momentum of migrating calcium ions are neglected, the balance of linear momentum is described by the vanishing divergence of the stress tensor σ:

$$\operatorname{div} q + [[\phi_0 + \phi_c]c]^{\cdot} + \dot{s} = 0, \qquad \operatorname{div} \sigma = 0 \tag{9}$$

The initial conditions, the Neumann and Dirichlet boundary conditions

$$
\begin{aligned}
c(t_0) &= c_0 \ \text{in} \ \Omega, & u(t_0) &= u_0 \ \text{in} \ \Omega \\
q \cdot n &= q^{\star} \ \text{on} \ \Gamma_q, & \sigma \cdot n &= t^{\star} \ \text{on} \ \Gamma_\sigma \\
c &= c^{\star} \ \text{on} \ \Gamma_c, & u &= u^{\star} \ \text{on} \ \Gamma_u
\end{aligned}
\tag{10}
$$

are given by Eqs. (10), where n is the normal vector on the boundary surface, $q^{\star}$ is the calcium ion mass flux across the chemical Neumann boundary Γ_q, $c^{\star}$ is the prescribed concentration on the chemical Dirichlet boundary Γ_c, $t^{\star}$ is the traction vector on the mechanical Neumann boundary Γ_σ, $u^{\star}$ is the prescribed displacement vector on the mechanical Dirichlet boundary Γ_u and t_0 is the initial time.

2.4. Constitutive laws

Taking the definition of the potential energy of the calcium ions and the strain energy of the deformed skeleton as the starting point, the calcium mass flux, the stress tensor, the dissipation inequalities and the equations governing the evolution of chemical matrix dissolution and mechanical damage are developed in the following.

2.4.1. Chemical potential and strain energy
The potential for the calcium ion transport Ψ_c within the pore space (volume fraction ϕ) and the strain energy Ψ_m related to the elastic deformation of the skeleton (volume fraction $1 - \phi$)

$$\Psi_c(\gamma, \phi_m, \phi_c) = \frac{\phi}{2}\gamma \cdot D_0 \cdot \gamma, \qquad \Psi_m(\varepsilon, \phi_m, \phi_c) = \frac{1 - \phi}{2}\varepsilon : \mathscr{C}_0 : \varepsilon \tag{11}$$

are defined in terms of the negative gradient of the calcium ion concentration field γ and the linear strain tensor ε:

$$\gamma = -\nabla c, \qquad \varepsilon = \nabla^{\text{sym}} \boldsymbol{u} = \tfrac{1}{2}[\nabla \boldsymbol{u} + \nabla^{\text{T}} \boldsymbol{u}] \tag{12}$$

Herein, $\boldsymbol{D}_0$ denotes the second order conductivity tensor of the pore fluid and $\mathscr{C}_0$ is the fourth order elasticity tensor of the skeleton. Consequently, the macroscopic conductivity and stiffness tensors of the porous material are given by $\boldsymbol{D} = \phi \boldsymbol{D}_0$ and $\mathscr{C} = [1 - \phi]\mathscr{C}_0$, respectively. $\phi = \phi_0$ defines the chemically and mechanically sound macroscopic material ($\phi_c = \phi_m = 0$), characterized by the subscript s. Hence, the macroscopic conductivity and stiffness tensors of the virgin material are given by $\boldsymbol{D}_s = \phi_0 \boldsymbol{D}_0$ and $\mathscr{C}_s = [1 - \phi_0]\mathscr{C}_0$. In contrast to existing reaction-diffusion models describing calcium leaching, the dependence of $\boldsymbol{D}_0$ on the square root of the calcium concentration within the pore fluid is considered. This dependency follows from Kohlrausch's law, describing the molar conductivity of strong electrolytes (see Atkins, 1998, and Section 3.1), using Nernst–Einstein's relation. In the isotropic case, the conductivity tensor $\boldsymbol{D}_0$ is given in terms of the second order identity tensor $\boldsymbol{1}$, the calcium ion conductivity for the infinitely diluted solution $D_{00} \geqslant 0$ and the constant $D_{0c} \geqslant 0$:

$$\boldsymbol{D}_0 = D_0 \boldsymbol{1} = [D_{00} - D_{0c}\sqrt{c}]\boldsymbol{1} \tag{13}$$

It can be observed, that the conductivity decreases with an increasing calcium concentration. This follows from the interaction of moving cations Ca^{2+} and anions OH^- by electrostatic forces and viscous forces. For $D_{0c} = 0$ Kohlrausch's law (13) degenerates to Fick's law (1855) of independent diffusing particles.

The strain energy includes the isotropic elasticity tensor of the skeleton, given in terms of the symmetric fourth order identity tensor $\mathscr{I}$, the Lamé constants μ_0 and λ_0 or, alternatively, by the Young's modulus E_0 and the Poisson ratio v:

$$\mathscr{C}_0 = 2\mu_0 \mathscr{I} + \lambda_0 \boldsymbol{1} \otimes \boldsymbol{1}, \qquad \lambda_0 = \frac{E_0 v}{[1 + v][1 - 2v]}, \quad \mu_0 = \frac{E_0}{2[1 + v]} \tag{14}$$

It should be noted, that the factor $\phi = \phi_0 + \phi_c + \phi_m$ in Eq. (11) takes into account, that the chemical potential Ψ_c is only related to the apparent pore space. The strain energy Ψ_m, on the other hand, is stored only in the skeleton. This is reflected by the factor $1 - \phi = 1 - \phi_0 - \phi_c - \phi_m$. Based on the definition of the chemical potential and the strain energy, the calcium ion mass flux vector, the stress tensor, the dissipations caused by damage and matrix dissolution, the Kuhn–Tucker conditions and the consistency conditions are now developed within the framework of thermodynamics.

2.4.2. Calcium ion mass flux vector and chemical dissipation

The calcium ion mass flux vector $\boldsymbol{q}$ is obtained as the derivative of the potential Ψ_c (11) with respect to the negative concentration gradient γ:

$$\boldsymbol{q} = \frac{\partial \Psi_c}{\partial \gamma} = \phi \boldsymbol{D}_0 \cdot \gamma \tag{15}$$

The rate of dissipated energy associated with the chemical dissolution process $\mathscr{D}_c = \mathscr{D}_{ct} + \mathscr{D}_{cc}$ is additively decomposed into a portion $\mathscr{D}_{ct}$ related to the transport of Ca^{2+} ions and a portion $\mathscr{D}_{cc}$ related to chemical dissolution, whereby each part must be non-negative (see Ulm et al., 1999):

$$\mathscr{D}_{ct} = RT\boldsymbol{q} \cdot \gamma \geqslant 0, \qquad \mathscr{D}_{cc} = A_s \dot{s} = \left[\mu_s - \frac{\partial \Psi_s}{\partial s}\right]\dot{s} \geqslant 0 \tag{16}$$

Herein, R and T are the universal gas constant and the total temperature, respectively. μ_s is the chemical potential per mole of the solute, $A_s = \mu_s - \partial \Psi_s / \partial s$ is the driving force of the calcium dissolution process,

denoted as chemical affinity and $\mu_{sc} = \partial \Psi_s / \partial s$ is the Gibbs potential of the skeleton. It is obvious, that the calcium leaching processes starts for $\dot{s} < 0$. According to inequality (16), this implies a negative chemical affinity $A_s < 0$.

2.4.3. Evolution of chemical matrix dissolution

The state of the chemically induced degradation of the skeleton is characterized by the calcium concentration s of the skeleton material. If chemical equilibrium between the calcium ions solved in the pore fluid and contained within the portlandite, ettringite and CSH-phases is assumed, the chemical dissolution process requires a decreasing calcium concentration of the pore fluid c. If, on the other hand, c is increased, the chemical structure of the skeleton is unchanged or, equivalently, the concentration s is constant. In contrast to existing models, this irreversible character of the cement dissociation is considered in the proposed model. Therefore, the internal variable κ_c, which represents the equilibrium concentration of bounded and dissolved calcium, is introduced. κ_c can be interpreted as the current threshold of the calcium concentration in the pore fluid with regards to chemical reactions. Based on the internal variable κ_c, the chemical reaction criterion is formulated:

$$\Phi_c = \kappa_c - c \leqslant 0 \tag{17}$$

Eqs. (16) and (17), and the principle of maximal dissipation (see e.g. Simo and Hughes, 1998) constitute a constraint optimization problem which yields the Kuhn–Tucker conditions and the consistency condition, describing the calcium dissolution:

$$\Phi_c \leqslant 0, \quad \dot{\kappa}_c \leqslant 0, \quad \Phi_c \dot{\kappa}_c = 0, \qquad \dot{\Phi}_c \dot{\kappa}_c = 0 \tag{18}$$

If the chemical reaction criterion (17) is violated, matrix dissolution sets in and the internal variable $\kappa_c = c$ is updated. Otherwise κ_c is unchanged and $\dot{\kappa}_c = 0$. As mentioned before, the internal parameter κ_c is related to the calcium concentration s of the skeleton. Assuming a chemical equilibrium state or, equivalently, instantaneous matrix dissolution, the phenomenological chemistry model proposed by Gérard (1996) and Delagrave et al. (1997) can be applied. This phenomenological chemistry model relates the concentration of dissolved calcium $s_0 - s$ to the chemical equilibrium concentration κ_c of calcium ions within the pore solution (see Fig. 3):

$$s_0 - s(\kappa_c) = [1 - \alpha_c] s_{\text{h}} \left[1 - \frac{\kappa_c}{10\bar{c}} + \frac{\kappa_c^2}{400\bar{c}^2} \right] + \frac{s_0 - s_{\text{h}}}{1 + \left[\frac{\kappa_c}{c_{\text{p}}} \right]^n} + \frac{\alpha_c s_{\text{h}}}{1 + \left[\frac{\kappa_c}{c_{\text{csh}}} \right]^m} \quad \text{for } 0 < \kappa_c < c_0$$

$$s_0 - s(\kappa_c) = 0 \quad \text{for } \kappa_c \geqslant c_0 \tag{19}$$

$$s_0 - s(\kappa_c) = s_0 \quad \text{for } \kappa_c \leqslant 0$$

In this function α_c, n, m are model parameters, c_0 and s_0 represent the equilibrium concentrations of the sound material, c_{p}, c_{csh} and s_{h} are material constants related to the averaged fluid calcium concentration associated with the dissolution of portlandite, the dissolution of CSH-phases and the solid calcium concentration associated with the portlandite free cement matrix and $\bar{c} = 1$ mol/m^3 is the physical dimension of κ_c. If the dissolved amount of cement constituents is calculated by Eq. (19), the related pore space can be determined by multiplying the amount of dissolved calcium $s_0 - s$ by the molar volume of the related constituents. To simplify the present model, the average molar volume $\mathcal{M}/\rho$ of portlandite, ettringite and CSH-phases is used:

$$\phi_c(s(\kappa_c)) = \frac{\mathcal{M}}{\rho} [s_0 - s(\kappa_c)] \tag{20}$$

Using the phenomenological chemical equilibrium (19), the matrix dissolution rate $\dot{s}$, constituting the source term of the calcium mass balance (9), is determined as a function of the concentration rate $\dot{c}$ by application of the chain rule:

$$\dot{s} = \frac{\partial s}{\partial \kappa_c} \dot{\kappa}_c = \frac{\partial s}{\partial \kappa_c} \frac{\partial \kappa_c}{\partial c} \dot{c} \tag{21}$$

The derivative $\partial s / \partial \kappa_c$ is given in Eq. (A.2). The derivative $\partial \kappa_c / \partial c$ is equal to one in the case of active matrix dissolution and zero otherwise:

$$\frac{\partial \kappa_c}{\partial c} = \begin{cases} 1 & \text{for } \Phi_c > 0, \ \dot{\kappa}_c < 0 \\ 0 & \text{for } \Phi_c \leqslant 0, \ \dot{\kappa}_c = 0 \end{cases} \tag{22}$$

Consequently, $\dot{s}$ is related to $\dot{c}$ in the case of matrix dissolution and zero if $c > \kappa_c$ holds.

2.4.4. Stress tensor and mechanical dissipation

The derivative of the strain energy (11) with respect to the strain tensor $\boldsymbol{\varepsilon}$ defines the stress tensor $\boldsymbol{\sigma}$:

$$\boldsymbol{\sigma} = \frac{\partial \Psi_m}{\partial \boldsymbol{\varepsilon}} = [1 - \phi]\mathscr{C}_0 : \boldsymbol{\varepsilon} = [1 - \phi_0 - \phi_c][1 - d_m]\mathscr{C}_0 : \boldsymbol{\varepsilon} \tag{23}$$

It is worth to note, that this result can be identically obtained from the theory of mixtures (Bowen, 1976), assuming the macroscopic material as a two-phase material. The two phases are the pore fluid with the volume fraction $\phi_0 + \phi_c$ and the mechanically damaged skeleton with the volume fraction $1 - \phi_0 - \phi_c$. According to damage theories (see e.g. Simo and Ju, 1987), the effective stress tensor of the skeleton is $[1 - d_m]\mathscr{C}_0 : \boldsymbol{\varepsilon}$. The conjugate thermodynamic force Y_m with regards to the damage parameter d_m is obtained by differentiation of the strain energy (11) with respect to the variable d_m:

$$Y_m = -\frac{\partial \Psi_m}{\partial d_m} = \frac{1 - \phi_0 - \phi_c}{2} \boldsymbol{\varepsilon} : \mathscr{C}_0 : \boldsymbol{\varepsilon} \tag{24}$$

Assuming isothermal conditions, the intrinsic dissipation

$$\mathscr{D}_m = -\frac{\partial \Psi_m}{\partial d_m} \dot{d}_m = Y_m \dot{d}_m \geqslant 0 \tag{25}$$

enforces a positive rate of mechanical damage $\dot{d}_m \geqslant 0$ for $Y_m \geqslant 0$.

2.4.5. Evolution of mechanical damage

The mathematical description of mechanical damage is a more or less classical topic extensively discussed in the literature (see e.g. Jirásek and Bažant, 2002; Krajcinovic, 1996; Lemaître, 1996; Lemaître and Chaboche, 1990). For the sake of completeness however, a brief review of the governing equations are given below. Adopting an isotropic damage model, material degradation is governed by the damage parameter $d_m(\kappa_m)$. According to Simo and Ju (1987), the damage criterion

$$\Phi_m = \eta(\boldsymbol{\varepsilon}) - \kappa_m \leqslant 0 \tag{26}$$

is employed. η denotes the equivalent strain function and κ_m is an internal damage variable defining the current damage threshold. The Kuhn–Tucker loading/unloading conditions and the consistency condition are obtained as a result of the constrained optimization problem constituted by Eqs. (25) and (26):

$$\Phi_m \leqslant 0, \quad \dot{\kappa}_m \geqslant 0, \quad \Phi_m \dot{\kappa}_m = 0, \qquad \dot{\Phi}_m \dot{\kappa}_m = 0 \tag{27}$$

From Eq. (27) follows, that κ_m is unchanged for $\Phi_m \leqslant 0$ and given by $\kappa_m = \eta$ otherwise:

$$\frac{\partial \kappa_m}{\partial \eta} = \begin{cases} 1 & \text{for } \Phi_m > 0, \;\; \dot{\kappa}_m > 0 \\ 0 & \text{for } \Phi_m \leqslant 0, \;\; \dot{\kappa}_m = 0 \end{cases} \tag{28}$$

To complete the description of the material model, the equivalent strain $\eta(\boldsymbol{\varepsilon})$ and the damage function $d_m(\kappa_m)$ must be defined. Here the equivalent strain measure proposed by Simo and Ju (1987)

$$\eta(\boldsymbol{\varepsilon}) = \sqrt{\frac{1}{E_0} \boldsymbol{\varepsilon} : \mathscr{C}_0 : \boldsymbol{\varepsilon}} \tag{29}$$

and the exponential damage function

$$d_m(\kappa_m) = 1 - \frac{\kappa_m^0}{\kappa_m}\left[1 - \alpha_m + \alpha_m \exp[\beta_m[\kappa_m^0 - \kappa_m]]\right] \tag{30}$$

are used, where κ_m^0 is the initial threshold and α_m, β_m are material parameters. It is worth to notice, that alternative equivalent strain functions, proposed e.g. by Mazars (1986) and de Vree et al. (1996), or alternative damage functions can be used for the constitutive modeling of materials in the framework of the proposed elasto-damage theory of porous media. In particular, the models referenced above are well suited for the modeling of concrete under compression as well as under tension.

2.4.6. Linearization of the constitutive laws

The linearization of the calcium mass flux vector $\boldsymbol{q}$ and the stress tensor $\boldsymbol{\sigma}$ with respect to the concentration c and the strain tensor $\boldsymbol{\varepsilon}$ is indispensable for a robust and effective finite element implementation of the proposed constitutive model. This yields the following expressions:

$$\Delta\boldsymbol{q} = \frac{\partial \boldsymbol{q}}{\partial c}\Delta c + \frac{\partial \boldsymbol{q}}{\partial \boldsymbol{\varepsilon}} : \Delta\boldsymbol{\varepsilon}, \qquad \Delta\boldsymbol{\sigma} = \frac{\partial \boldsymbol{\sigma}}{\partial c}\Delta c + \frac{\partial \boldsymbol{\sigma}}{\partial \boldsymbol{\varepsilon}} : \Delta\boldsymbol{\varepsilon} \tag{31}$$

where, for example, $\partial\boldsymbol{q}/\partial\boldsymbol{\varepsilon} : \Delta\boldsymbol{\varepsilon}$ represents the Gâteaux derivative of the calcium mass flux vector $\boldsymbol{q}$ in direction of the strain increment $\Delta\boldsymbol{\varepsilon}$. Details of the above derivatives, namely the Gâteaux derivatives $\partial\boldsymbol{q}/\partial c\Delta c$, $\partial\boldsymbol{q}/\partial\boldsymbol{\varepsilon} : \Delta\boldsymbol{\varepsilon}$, $\partial\boldsymbol{\sigma}/\partial c\Delta c$ and $\partial\boldsymbol{\sigma}/\partial\boldsymbol{\varepsilon} : \Delta\boldsymbol{\varepsilon}$, are given in Appendix A.

2.5. Synopsis and relation to existing models

The proposed thermodynamic model for coupled chemo-mechanical deterioration of cementitious materials is summarized in Table 2. It is obvious, that the interaction of mechanical and chemical induced damage is governed by the total porosity, defined in terms of the initial porosity, the chemically induced porosity and the mechanically induced apparent porosity. Based on the total porosity, the chemical as well as the mechanical properties are derived without further assumptions or empirical models within the framework of the theory of mixtures (Bowen, 1976). The irreversible character of matrix dissolution and mechanical damage is considered by internal variables defined in a complete equivalent form. Using a damage as well as a chemical reaction criterion, conditions for propagating matrix dissolution and mechanical damage are consistently derived within a unified thermodynamic framework.

Table 3 contains a comparison of existing models describing chemo-mechanical damage of concrete, based upon the work by Gérard (1996), Delagrave et al. (1997) and Gérard et al. (1998) and applied to coupled chemo-mechanical structural analyses (Arroyo et al., 2000; Le Bellégo et al., 2000, 2001a,b; Díez et al., 2002; Gérard, 2000; Gérard et al., 1998; Pijaudier-Cabot et al., 1998a,b, 2002) with the proposed chemo-mechanical damage model. A common aspect in both models is the assumption of an instantaneous matrix dissolution, reflected in the phenomenological equilibrium chemistry model by Gérard (1996) and

Delagrave et al. (1997). Important differences are related to the derivation of constitutive laws. In the proposed model, a uniform theory for the coupled chemo-mechanical problem based upon the total porosity and the theory of mixtures is developed, whereas in the existing models constitutive laws for the mechanical and the chemical sub-problem are defined and identified separately from experimental results. A chemical internal variable is introduced in the proposed model which allows the derivation of the chemical reaction criteria (17) and (18) and consideration of cyclic chemical loading.

These criteria for propagating dissociation of the cement skeleton, developed within the framework of thermodynamics, are compared with reaction criteria proposed by Mainguy and Coussy (2000) based on the analysis of the chemical system. Using the notation of the present paper, these criteria for propagating matrix dissolution have the form:

$$c - c^{\text{eq}} \leqslant 0, \quad \dot{s} \geqslant 0, \quad [c - c^{\text{eq}}]\dot{s} = 0 \tag{32}$$

c^{eq} represents the current equilibrium concentration equivalent to κ_c and $\dot{s}$ is calcium mass rate given by Eqs. (21) and (A.2) as $\dot{s} = -\dot{\kappa}_c \mathcal{M}/\rho$. Hence, the conditions for chemical reactions proposed by Mainguy and Coussy (2000) and the damage criteria (17) and (18) proposed in the present paper are identical, although their derivations are different.

3. Model studies on reaction-diffusion and chemo-mechanical couplings

This section contains model studies to illustrate the main features of the proposed chemo-mechanical damage model with regards to chemical dissolution, mechanical damage and the interaction of chemical and mechanical processes. The results are compared to existing models and experiments. In Section 3.1, the conductivity constants concerning the migration of Ca^{2+} ions are determined according to the theory of strong electrolytes. A comparison between the phenomenological equilibrium chemistry model and alternative models as well as experimental results is given in Section 3.2. In Section 3.3 the character of mechanically induced porosity is investigated. As a main aspect of the model the influence of chemo-mechanical damage on the diffusivity, stiffness and strength of cementitious materials is investigated and compared to experimental results in Section 3.4. Finally, the behavior of the model under cyclic chemical and mechanical conditions is studied (Section 3.6) and a dimensional analysis of source/storage terms is performed (Section 3.7). Material and model parameters used in the studies are given in Table 1. The Lamé constants correspond to Young's modulus of concrete on a macroscopic level $E_s = [1 - \phi_0]E_0 = 35 \times 10^9$ N/m^2 and the Poisson's ratio $v = 0.2$. The parameters describing the phenomenological equilibrium between calcium of the skeleton and the interstitial pore solution are chosen according to Gérard (1996) and Delagrave et al. (1997).

3.1. Migration of calcium ions in water and electrolyte solutions

It is widely accepted, that calcium leaching in cementitious porous materials is mainly controlled by the transport properties of the pore fluid and the volume fraction of the pore space (see e.g. Adenot, 1992;

Table 1
Material and model parameters

$\lambda_0 = 12.153 \times 10^9$ N/m^2	$c_0 = 20.7378$ mol/m^3	$n = 85$
$\mu_0 = 18.229 \times 10^9$ N/m^2	$c_{\text{p}} = 19$ mol/m^3	$m = 5$
$\phi_0 = 0.2$	$c_{\text{csh}} = 1.5$ mol/m^3	$\frac{\mathcal{M}}{\rho} = 3.5 \times 10^{-5}$ m^3/mol
$\kappa_m^0 = 1.1 \times 10^{-4}$	$s_0 = 15$ kmol/m^3	$D_{00} = 791.8 \times 10^{-12}$ m^2/s
$\alpha_m = 0.9$	$s_{\text{h}} = 9$ kmol/m^3	$D_{0c} = 96.85 \times 10^{-12}$ m^2/s $\sqrt{\text{m}^3/\text{mol}}$
$\beta_m = 1000$	$\alpha_c = 0.565$	

Table 2
Summary of the ingredients of the proposed thermodynamic model for coupled chemo-mechanical damage of cementitious materials

Chemistry	Mechanics
Initial boundary value problems	
Mass balance of the solute	Balance of linear momentum
$\operatorname{div} \boldsymbol{q} + [[\phi_0 + \phi_c]c]^{\cdot} + \dot{s} = 0$ in Ω	$\operatorname{div} \boldsymbol{\sigma} = \boldsymbol{0}$ in Ω
Neumann boundary condition	Neumann boundary condition
$\boldsymbol{q} \cdot \boldsymbol{n} = q^{\star}$ on Γ_q	$\boldsymbol{\sigma} \cdot \boldsymbol{n} = \boldsymbol{t}^{\star}$ on Γ_σ
Dirichlet boundary condition	Dirichlet boundary condition
$c = c^{\star}$ on Γ_c	$\boldsymbol{u} = \boldsymbol{u}^{\star}$ on Γ_u
Initial condition	Initial condition
$c(t=0) = c_0^{\star}$ in Ω	$\boldsymbol{u}(t=0) = \boldsymbol{u}_0^{\star}$ in Ω
Total porosity, $\phi = \phi_0 + \phi_c + \phi_m$	
Chemically induced porosity	Apparent mechanically induced porosity
$\phi_c = \frac{\mathscr{M}}{\rho}[s_0 - s]$	$\phi_m = [1 - \phi_0 - \phi_c]d_m$
Apparent porosity	Apparent volume fraction of the skeleton
$\phi = [\phi_0 + \phi_c][1 - d_m] + d_m$	$1 - \phi = [1 - \phi_0 - \phi_c][1 - d_m]$
Volume fraction of the pore space	Volume fraction of the skeleton
$\phi_0 + \phi_c = \phi - \phi_m$	$1 - \phi_0 - \phi_c = 1 - \phi + \phi_m$
Constitutive laws	
Potential of calcium ion transport	Strain energy of deformed skeleton
$\Psi_c = \frac{\phi}{2}\boldsymbol{\gamma} \cdot \boldsymbol{D}_0 \cdot \boldsymbol{\gamma}$	$\Psi_m = \frac{1-\phi}{2}\boldsymbol{\varepsilon} : \mathscr{C}_0 : \boldsymbol{\varepsilon}$
Concentration gradient	Linearized strain tensor
$\boldsymbol{\gamma} = -\nabla c$	$\boldsymbol{\varepsilon} = \nabla^{\text{sym}}\boldsymbol{u} = \frac{1}{2}[\nabla \boldsymbol{u} + \nabla^{\text{T}}\boldsymbol{u}]$
Conductivity tensor of the pore fluid	Elasticity tensor of the skeleton
$\boldsymbol{D}_0 = [D_{00} - D_{0c}\sqrt{c}]\mathbf{1}$	$\mathscr{C}_0 = 2\mu_0 \mathscr{I} + \lambda_0 \mathbf{1} \otimes \mathbf{1}$
Macroscopic solute flux vector	Macroscopic stress tensor
$\boldsymbol{q} = \phi \boldsymbol{D}_0 \cdot \boldsymbol{\gamma}$	$\boldsymbol{\sigma} = [1 - \phi]\mathscr{C}_0 : \boldsymbol{\varepsilon}$
Constitutive laws—damage evolutions	
Chemical reaction criterion	Damage criterion
$\Phi_c = \kappa_c - c \leqslant 0$	$\Phi_m = \eta(\boldsymbol{\varepsilon}) - \kappa_m \leqslant 0$
Kuhn–Tucker and consistency conditions	Kuhn–Tucker and consistency conditions
$\Phi_c \leqslant 0,\ \dot{\kappa}_c \leqslant 0,\ \Phi_c \dot{\kappa}_c = 0,\ \dot{\Phi}_c \dot{\kappa}_c = 0$	$\Phi_m \leqslant 0,\ \dot{\kappa}_m \geqslant 0,\ \Phi_m \dot{\kappa}_m = 0,\ \dot{\Phi}_m \dot{\kappa}_m = 0$
	Equivalent strain (29)
	$\eta = \eta(\boldsymbol{\varepsilon})$
Chemical porosity function (19) and (20)	Damage function (30)
$\phi_c = \phi_c(s(\kappa_c))$	$d_m = d_m(\kappa_m)$
Constitutive laws—dissipation inequalities	
	Thermodynamic force
	$Y_m = \frac{1-\phi_0-\phi_c}{2}\boldsymbol{\varepsilon} : \mathscr{C}_0 : \boldsymbol{\epsilon}$
Transport dissipation rate	Mechanical dissipation rate
$\mathscr{D}_{ct} = RT\boldsymbol{q} \cdot \boldsymbol{\gamma} \geqslant 0$	$\mathscr{D}_m = Y_m \dot{d}_m \geqslant 0$
Chemical dissolution dissipation rate	
$\mathscr{D}_{cc} = \left[\mu_s - \frac{\partial \Psi_s}{\partial s}\right]\dot{s} \geqslant 0$	

Carde and François, 1997; Delagrave et al., 1997; Gérard, 1996; Gérard et al., 1998; Heukamp et al., 2001b; Le Bellégo et al., 2000; Mainguy and Coussy, 2000; Mainguy and Ulm, 2000; Ulm et al., 1999). Due to the crucial role of transport mechanisms, the migration of calcium ions Ca^{2+} in pure water and in strong electrolyte solutions is investigated within this subsection. The conductivity is estimated based upon molecular mobility of calcium ions in water according to Atkins (1998). For the sake of simplicity an univalent double charged electrolyte solution is assumed. The conductivity $\boldsymbol{D}_0$ can be calculated based on the molar conductivity Λ by application of the Nernst–Einstein relation. Strictly speaking, this relation is restricted to

infinitely diluted solutions. It may serve, however, as an approximation for concentrated solutions. The molar conductivity Λ of a strongly electrolyte solution is given as function of the calcium ion concentration in the pore fluid c by the empirical Kohlrausch law (see Kohlrausch, 1900):

$$\boldsymbol{D}_0 = D_0 \mathbf{1} = \frac{RT}{z^2 F^2} \Lambda \mathbf{1}, \quad \Lambda = \Lambda_0 - \Lambda_c \sqrt{c} \tag{33}$$

Herein, $R = 8.31451$ J/K mol is the universal gas constant, T is the total temperature chosen as $T = 298$ K, $z = 2$ is the number of elementary charges of a cation Ca^{2+}, $F = 9.64853 \times 10^4$ C/mol is the Faraday constant, $\Lambda_0 = 11.9 \times 10^{-3}$ S m²/mol is the molar conductivity at infinite dilution and Λ_c is the Kohlrausch constant of the molar conductivity. Based upon the model of ionic clouds, the Debye–Hückel–Onsager theory (Debye and Hückel, 1923; Onsager, 1927) verifies Kohlrausch's law and allows to determine the Kohlrausch constant Λ_c,

$$\Lambda_c = A + B\Lambda_0, \quad A = \frac{z^2 e F^2}{3\pi\eta} \sqrt{\frac{2}{\epsilon RT}}, \quad B = \frac{q z^3 e F^2}{24\pi\eta RT} \sqrt{\frac{2}{\epsilon RT}} \tag{34}$$

where the constants A and B account for electrophoretic and relaxation effects associated with the ion–ion interactions. These constants are given in terms of the universal gas constant, the total temperature, the elementary charge $e = 1.602177 \times 10^{-19}$ C, the constant $q = 0.586$, the electric permittivity $\epsilon = 6.954 \times 10^{-10}$ C²/J m and the viscosity $\eta = 0.891 \times 10^{-3}$ kg/ms of water (see e.g. Atkins, 1998). From comparing Eqs. (13) and (33) the macroscopic diffusion constants D_{00} and D_{0c} can be determined:

$$D_{00} = \frac{RT}{z^2 F^2} \Lambda_0 = 791.8 \times 10^{-12} \; \frac{\text{m}^2}{\text{s}}, \qquad D_{0c} = \frac{RT}{z^2 F^2} \Lambda_c = 96.85 \times 10^{-12} \; \frac{\text{m}^2}{\text{s}} \sqrt{\frac{\text{m}^3}{\text{mol}}} \tag{35}$$

In the present model the macroscopic diffusion coefficient ϕD_0 can be determined for any state of chemo-mechanical degradation characterized by the history variables κ_c and κ_m and for any concentration c.

Fig. 2 contains plots of the conductivity D_0 in the pore fluid and the macroscopic conductivity ϕD_0 vs. the calcium concentration within the range $c = 0$ corresponding to pure water and $c = c_0$ corresponding to the concentrated pore solution of the virgin material. The diagrams on the left-hand side of Fig. 2 underline the relevance of using higher order ion transport models, considering electrophoretic and
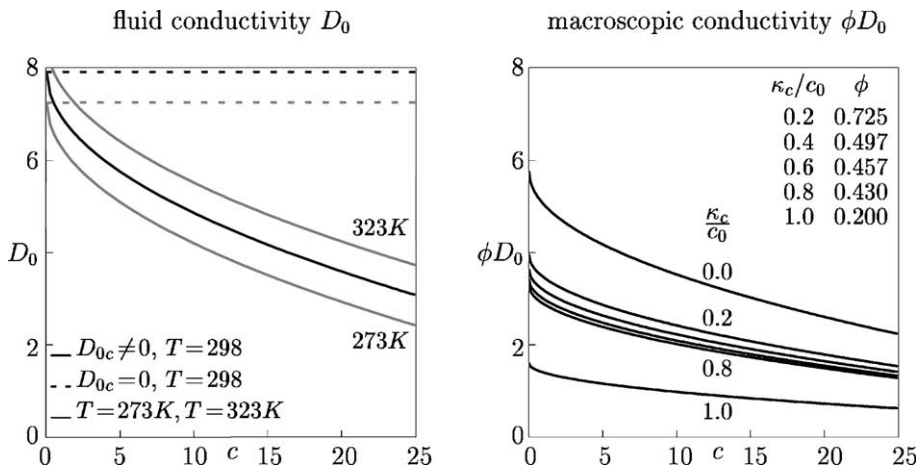

Fig. 2. Conductivity of the pore fluid D_0 [10^{-10} m²/s] as function of the calcium concentration c [mol/m³] and the total temperature T [K]. Macroscopic conductivity of non-reactive porous media ϕD_0 [10^{-10} m²/s] as function of the calcium concentration c [mol/m³] and the porosity ϕ [–] with $\phi = \phi(\kappa_c, d_m = 0)$.

relaxation effects, as a basis for realistic calcium leaching models. Standard and higher order transport models are characterized by $D_{0c} = 0$ and $D_{0c} \neq 0$, respectively. A pronounced change of the conductivity D_0 proportional to the square root of the concentration c can be observed within the considered concentration range. The ratio of the conductivities related to the fully degraded material $D_0(0)$ and the virgin material $D_0(c_0)$ is approximately 9:4. The average value of the conductivity D_0 is approximately $D_0 \approx 4 \times 10^{-10}$ m/s^2. This is in accordance with the suggestion by Delagrave et al. (1997), that in numerical analyses $D_0/2$ should be used as the macroscopic conductivity in order to fit experimental results. Standard transport models are not capable to capture the significant increase of the conductivity with a decreasing calcium ion concentration corresponding to propagating chemical damage in reactive porous media. As expected, the results of the standard model and the present model are identical in the case of infinitely diluted solutions ($c = 0$). The sensitivity of the ion transport with regards to temperature changes is studied by including plots of the conductivity for $T = 273$ K, corresponding to the freezing point of water (no calcium ion transport occurs below this temperature), and for $T = 323$ K, representing approximately a desert climate, in Fig. 2. According to Eqs. (13) and (35), the conductivity D_0 depends linearly on the total temperature T. Within the considered temperature interval D_0 is only changed by approximately 16%. Compared to the influence of the concentration the influence of the temperature plays a minor role in the transport process of ions within the pore water of cementitious materials.

On the right-hand side of Fig. 2, the macroscopic conductivity is plotted for various values of the threshold calcium concentration κ_c and the corresponding values of the porosity, respectively, assuming a non-reactive porous material.

3.2. Phenomenological chemistry

In the proposed chemo-mechanical damage model, the reaction-diffusion problem of calcium leaching is controlled by the phenomenological chemical equilibrium function (19). This function is originally proposed by Delagrave et al. (1997) and Gérard (1996) on the basis of experimental results by Berner (1988, 1992). This relation controls the skeleton calcium concentration s, the dissolution rate $\dot{s}$, the chemically introduced porosity ϕ_c and, consequently, the macroscopic transport and mechanical properties of the material. Plots of the function (19) and their derivatives with respect to the internal variable κ_c are
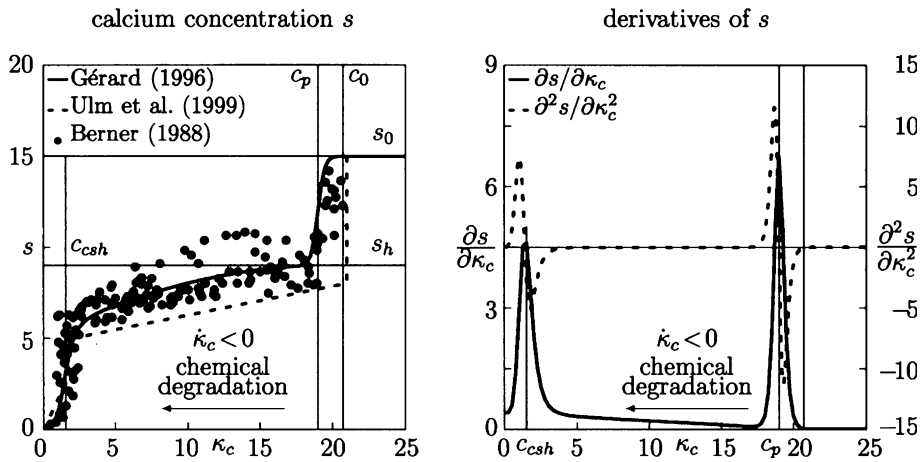

Fig. 3. Relations between s and κ_c and their derivatives based on the phenomenological chemistry model by Gérard (1996) and experimental results by Berner (1988). $s(\kappa_c)$ [kmol/m^3] and its derivatives $\partial s(\kappa_c)/\partial \kappa_c$ [10^3] and $\partial^2 s(\kappa_c)/\partial \kappa_c^2$ [m^3/mmol] as functions of κ_c [mol/m^3].

contained in Fig. 3. Increasing chemical damage is characterized by $\dot{\kappa}_c < 0$. The smooth steps of function $s(\kappa_c)$ at $\kappa_c \approx c_p$ and $\kappa_c \approx c_{csh}$ correspond to the dissolution of calcium hydroxide (portlandite) and CSH-phases, respectively. Ettringite is dissolved within the range between this two dissolution fronts (4 mol/m^3 < κ_c < 18 mol/m^3). The $s(\kappa_c)$-curve is compared to experimental results by Berner (1988, 1992) and to a simplified phenomenological chemical equilibrium model proposed by Ulm et al. (1999). Both models replicate the experimental data with sufficient accuracy. They are successfully applied to calcium leaching (see e.g. Arroyo et al., 2000; Le Bellégo et al., 2000, 2001a; Delagrave et al., 1997; Díez et al., 2002; Gérard, 1996, 2000; Gérard et al., 1998; Kuhl et al., 2000; Pijaudier-Cabot et al., 1998a,b, 2002; Mainguy, 1999; Mainguy and Coussy, 2000; Mainguy et al., 2000, 2001; Mainguy and Ulm, 2000; Ulm et al., 2001). As far as numerical and algorithmic aspects are concerned, the main advantage of Gérard's model (1996) is the C_2-continuity of the $s(\kappa_c)$-curve. As a consequence, the source terms $\dot{s}$ and $\dot{c}$ can be related in a consistent manner by application of the chain rule (see Eq. (21)). Furthermore, consideration of different cases within the numerical analysis of the reaction-diffusion problem is avoided. The curve $\partial s/\partial \kappa_c$ and, consequently, the source term $\dot{s}$ (21) are characterized by pronounced peaks at the dissolution fronts of calcium hydroxide and CSH-phases, respectively. Since the second derivative of $s(\kappa_c)$ is required for the calculation of the consistently linearized tangent matrix (see the second part of the present paper, Kuhl et al., in press), it is also included in Fig. 3. $\partial^2 s/\partial \kappa_c^2$ strongly oscillates at $\kappa_c = c_p$ and $\kappa_c = c_{csh}$. Hence, the tangent operator is expected to be highly sensitive to variations of the calcium concentration c.

3.3. Total and apparent mechanical porosity

The left-hand side of Fig. 4 illustrates the dependence of the total porosity ϕ of reactive porous materials on the dissolution threshold κ_c and on the mechanical damage parameter d_m according to Eqs. (19) and (20). In this figure the results from the present model are compared with the models proposed by Gérard (1996) and by Ulm et al. (1999). These porosity models only consider the initial and the chemically induced porosity, while the present model also takes mechanically induced pores and micro-cracks into account. In Gérard's model and in the present model, the chemically induced porosity depends linearly on the dissolved moles of calcium $s_0 - s$ with the molar volume of the skeleton material as proportionality factor. The empirical model proposed by Ulm et al. (1999) is based on measured data $\phi(c)$. Due to the very fine CSH
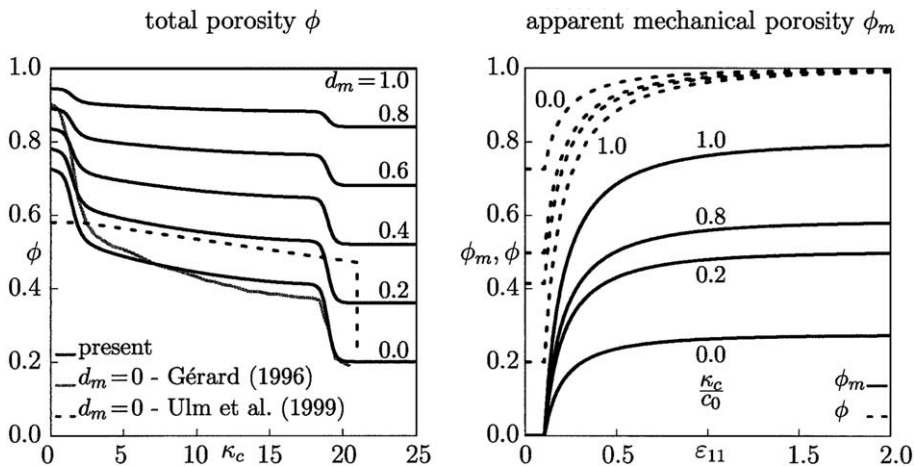

Fig. 4. Total porosity $\phi(\kappa_c, d_m)$ [–] and apparent mechanical porosity $\phi_m(\kappa_c, d_m)$ [–] as functions of the chemical degradation κ_c [mol/m^3], the mechanical damage parameter d_m [–] and the prescribed normal strain ε_{11} [10^3].

crystals (see e.g. Taylor, 1997), the porosity due to the dissolution of CSH-phases is neglected in this model. With regards to chemically induced porosity, the differences between the three models are relatively small. In contrast to existing models, the present model accounts for the creation of the apparent pore space due to mechanical damage. From Fig. 4 it can be observed, that mechanical damage significantly influences the total porosity ϕ. It depends on the scalar damage parameter d_m, with $d_m = 1$ representing a fully damaged skeleton associated with $\phi = 1$.

The right-hand side of Fig. 4 illustrates the porosities ϕ_m and ϕ as functions of ε_{ij} assuming one-dimensional loading. If the equivalent strain measure $\eta = \varepsilon_{11}$ exceeds the initial damage threshold κ_m^0, an increasing ε_{11} is correlated with increasing mechanical damage d_m. For a constant level of κ_c the apparent mechanical porosity ϕ_m follows the damage evolution law (30) scaled by the factor $1 - \phi_0 - \phi_c$. It is interesting to note, that according to the proposed chemo-mechanical model, the mechanical porosity ϕ_m is reduced as chemical damage increases. This accounts for the chemical dissolution of mechanically damaged material, whereby the apparent mechanical porosity is transformed to chemical porosity. The dashed lines in the right-hand side of Fig. 4 represent the total porosity. They show, that the total porosity increases with chemical as well as mechanical damage. With increasing mechanical damage, the differences between sound and chemically degraded materials vanishes. This means, that the total porosity is dominated by mechanical damage for high levels of the damage parameter d_m and, vice versa, dominated by matrix dissolution for low levels of mechanical damage. This observation is indirectly confirmed by the empirical calcium mass transport model by Gérard (1996), Gérard et al. (1998), Pijaudier-Cabot et al. (1998a,b) and Le Bellégo et al. (2000) (see Table 3) which is based on experimental results. In this model the influence of chemically induced porosity on the mass flux is neglected for high levels of mechanical damage. For low levels of the damage parameter d_m the influence of mechanical damage on the mass flux is neglected (compare Table 3).

3.4. Influence of chemical dissolution and damage on the conductivity

On the left-hand side of Fig. 5 the macroscopic conductivity ϕD_0 obtained from standard transport models and from the proposed transport model is plotted as a function of the dissolution threshold κ_c and the damage parameter d_m. The dashed lines are obtained from standard ion transport models ($D_{0c} = 0$). Since the conductivity ϕD_0 is a linear function of the porosity, these curves are similar to the graphs of the total porosity in Fig. 4. The solid lines are obtained from the present higher order ion transport model. According to this model, the conductivity is increased for increasing damage and matrix dissolution. $d_m = 1$ corresponds to the macroscopic counterpart of Kohlrausch's law given by Eq. (13). The pronounced steps in the ϕD_0-curves, associated with the dissolution fronts of portlandite and CSH-phases, are smoothened at higher levels of mechanical damage. The reason for the smoothening is the dominance of mechanical damage in this range. The increase of the macroscopic conductivity with propagating calcium leaching and mechanical damage has been shown in experiments by Adenot (1992) and Gérard (1996), respectively.

The macroscopic calcium ion conductivity ϕD_0 of reactive porous materials is plotted on the right-hand side of Fig. 5 as function of the total porosity ϕ. The relations between ϕ, c and d_m according to Eqs. (4), (17), (19) and (20), assuming monotonously increasing chemical damage, characterized by $\kappa_c = c$, are used. The linear functions ϕD_{00} and $\phi D_0(c_0) = \phi[D_{00} - D_{0c}\sqrt{c_0}]$ corresponding to the standard transport model and to the proposed higher order model for chemically sound materials are the upper and lower bounds of the macroscopic conductivity. With increasing mechanical damage, the error made by applying the standard transport model increases. For fully chemically degraded materials, with the calcium concentration in the pore fluid approaching to zero and the ions migrating independently in the pore fluid, both models yield identical results. Fig. 5 also includes least square fits of the curves $\phi D_0(\phi)$ of the exponential type $D(\phi) = a \exp[b\phi]$. The curves for $d_m = 0.0$, 0.4, 0.8 were obtained using the parameters $10^{12}a = 45.4$, 19.2, 0.072 m^2/s and $b = 3.5$, 4.2, 9.8. It is noteworthy, that for the interpretation of measurements by e.g. Adenot (1992), Adenot and Buil (1992), Mainguy et al. (2000), and Le Bellégo et al. (2001a) also an

Table 3
Comparison between existing models and the proposed chemo-mechanical model

Existing models	Present model
Stress tensor	
$\boldsymbol{\sigma} = [1 - V][1 - d_m]\mathscr{C} : \boldsymbol{\varepsilon}$, $\mathscr{C} = [1 - \phi_0]\mathscr{C}_0$	$\boldsymbol{\sigma} = [1 - \phi_0 - \phi_c][1 - d_m]\mathscr{C}_0 : \boldsymbol{\varepsilon}$
• Empirical calculation of $V(c)$	• ϕ_0 and ϕ_c equivalent types of porosity
• Damage of the macroscopic material, equivalent strain by Mazars (1986)	• Damage restricted to the skeleton, equivalent strain by Simo and Ju (1987)
	• Chemo-mechanical interaction based on theory of mixtures
Mass flux vector	
$\boldsymbol{q} = \max(D(d_m), D(c))\boldsymbol{\gamma}$	$\boldsymbol{q} = [\phi_0 + \phi_c + \phi_m]\boldsymbol{D}_0(c) \cdot \boldsymbol{\gamma}$
• Empirical determination of $D(d_m)$ and $D(c)$	• $\boldsymbol{D}_0$ based on theory of electrolytes
• No interaction of chemical and mechanical damage	• Interaction of chemical and mechanical damage due to the theory of mixtures
Chemical reaction, reaction criterion and mass balance	
$s = s(c)$, $\dot{s} = \frac{\partial s}{\partial c}\dot{c}$	$s = s(\kappa_c)$, $\dot{s} = \frac{\partial s}{\partial \kappa_c}\frac{\partial \kappa_c}{\partial c}\dot{c}$
• Phenomenological equilibrium chemistry by Gérard (1996): $s(c)$	• Phenomenological equilibrium chemistry by Gérard (1996): $s(\kappa_c)$
• $\dot{s}$ as function of $\dot{c}$, applying chain rule	• $\dot{s}$ as function of $\dot{c}$, applying chain rule
	$\Phi_c \leqslant 0$, $\dot{\kappa}_c \leqslant 0$, $\Phi_c\dot{\kappa}_c = 0$
• No reaction criterion, no internal variable	• Reaction criterion and internal variable κ_c
	• Reaction conditions (Kuhn–Tucker)
$\operatorname{div}\boldsymbol{q} + \dot{s} = 0$	$\operatorname{div}\boldsymbol{q} + [[\phi_0 + \phi_c]c]^{\cdot} + \dot{s} = 0$
• Neglecting the term $[[\phi_0 + \phi_c]c]^{\cdot}$	• Considering the term $[[\phi_0 + \phi_c]c]^{\cdot}$
• Only proportional chemical loading	• Allows together with κ_c for cyclic loading
Evolution of porosity	
$\phi(c) = \phi_0 + \sum_i \frac{\mathscr{M}_i}{\rho_i}[s_0 - s_i(c)] = \phi_0 + \phi_c$	$\phi_c(s(\kappa_c)) = \frac{\mathscr{M}}{\rho}[s_0 - s(\kappa_c)]$
• Calculation of the porosity from the individual dissolved phases	• Calculation of average value of the porosity from dissolved portlandite, ettringite and CSH
Literature and first ideas	
Gérard (1996)	Kuhl et al. (2000)
Delagrave et al. (1997)	Bangert et al. (2001)
Gérard et al. (1998)	Proposed model
Pijaudier-Cabot et al. (1998a,b)	
Le Bellégo et al. (2000, 2003)	

exponential function was used to fit the experimental data. The present study demonstrates, however, that the macroscopic conductivity is governed by three interacting physical, electro-chemical and chemical mechanisms which cannot be separated in the experiments: Firstly, the transport of ions through the pore space for a constant calcium concentration, represented by the theory of mixtures as a linear function of the porosity. Secondly, the dependence of the conductivity of the pore fluid on the square root of the calcium concentration (compare Fig. 2) due to electrophoretic and relaxation effects. And finally, the increasing pore space associated with a decreasing calcium concentration due to the chemical reaction of the skeleton and the solute.

3.5. Influence of chemical dissolution and damage on stiffness and strength

The influence of chemical degradation on the material stiffness is investigated next. Fig. 6 shows the normalized stiffness, i.e. the ratio of the current macroscopic Young's modulus E and the Young's modulus of the sound macroscopic material E_s (compare Eq. (23))
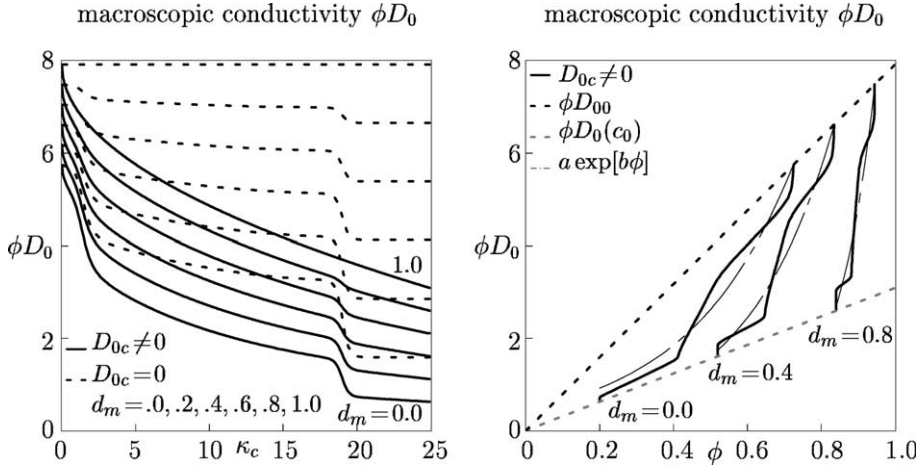
Fig. 5. Macroscopic conductivity ϕD_0 [10^{-10} m^2/s] with $c = \kappa_c$ as function of the chemical degradation κ_c [mol/m^3] and the mechanical damage parameter d_m [–].
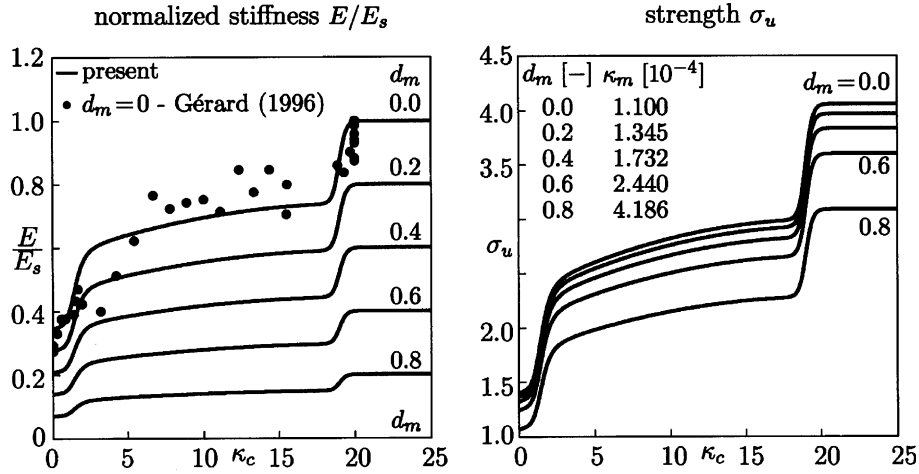

Fig. 6. Normalized stiffness E/E_s [–] and strength σ_u [N/mm^2] as function of the chemical degradation κ_c [mol/m^3] and the mechanical damage parameter d_m [–].

$$\frac{E}{E_s} = \frac{[1-\phi]E_0}{[1-\phi_0]E_0} = \frac{1-\phi}{1-\phi_0} \tag{36}$$

as a function of the state of chemical and mechanical degradation characterized by κ_c and d_m. A comparison of the purely chemical model ($d_m = 0$) with experimental results by Gérard (1996) shows a good correlation between the model and experimental data. In particular, the influence of the dissolution of portlandite and CSH-phases on the stiffness of the material observed from the experimental data is replicated well by the present model.

The influence of chemically and mechanically induced damage on the strength of the material is investigated next. According to the proposed chemo-mechanical model, the current residual strength

$\sigma_u(\kappa_c, \kappa_m)$ of a chemo-mechanical degraded porous material is controlled by the damage criterion (26), the equivalent strain (29), the current damage threshold (26) $\eta(\varepsilon) = \kappa_m$

$$\eta(\varepsilon_{11}) = \varepsilon_{11}\sqrt{\frac{[1+v][1-2v]}{1-v}} = \kappa_m \tag{37}$$

and the homogenization of the effective stress of the skeleton on the basis of the theory of mixtures:

$$\sigma_u(\kappa_c, \kappa_m) = [1 - \phi(\kappa_c, \kappa_m)]E_0\kappa_m\sqrt{\frac{1-v}{[1+v][1-2v]}} \tag{38}$$

The right-hand side of Fig. 6 contains the strength σ_u as a function of the dissolution κ_c and the mechanical damage parameter d_m. κ_m in Eq. (38) is determined from d_m by inverting Eq. (30). It can be observed, that the strength of the material decreases with increasing chemical and mechanical damage. In particular, the dissolution of portlandite and CSH-phases significantly reduces the strength of the material.

Both effects of calcium leaching on the mechanical properties, namely the reduction of stiffness and strength, are confirmed by experimental results reported by Carde et al. (1996, 1997a,b), Carde and François (1997), Le Bellégo et al. (2000, 2001a,b) and Heukamp et al. (2001a).

3.6. Cyclic chemical and mechanical loading

The next model study is concerned with the behavior of the present model under cyclic chemical and mechanical loading. In the numerical studies, cyclic chemical loading is accomplished by a step-wise reduction of the concentration c. Starting with $c = 25$ mol/m³, the concentration is reduced to $c = 0.8c_0$, increased to the initial value, reduced to $c = 0.4c_0$, increased again to the initial value and finally reduced to $c = 0$. Cyclic mechanical loading is accomplished by increasing and decreasing the strain $\varepsilon_{11} = 0.002$ in three loading–unloading cycles. Plots of the macroscopic conductivity ϕD_0 and of the stress σ_{11} as functions of the prescribed concentration c and strain ε_{11}, respectively, are given in Fig. 7 for different levels of mechanical and chemical degradation represented by d_m and κ_c/c_0. For loading processes, the ϕD_0-curves shown in Fig. 7 are identical to the related curves given in Fig. 5. In chemical unloading processes, however,
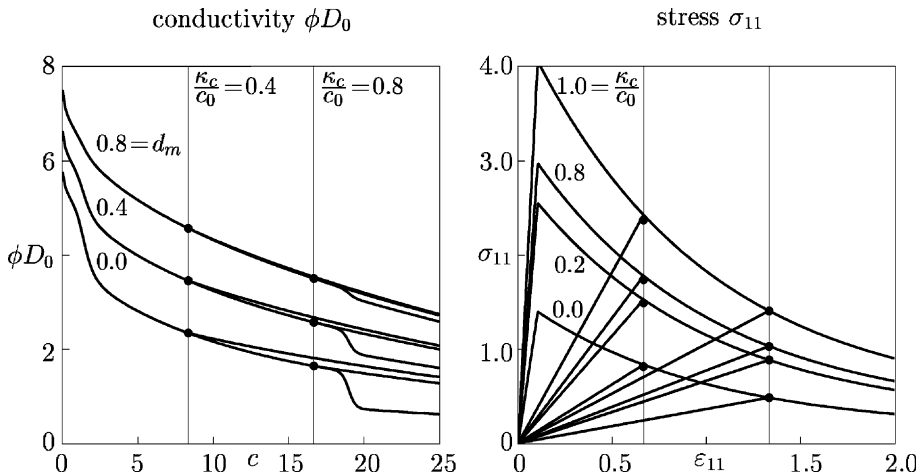

Fig. 7. Cyclic chemical loading: conductivity ϕD_0 [10^{-10} m²/s] as a function of the prescribed concentration of the pore fluid c [mol/m³]. Cyclic mechanical loading: Normal stress σ_{11} [N/mm²] as a function of the prescribed strain component ε_{11} [10^{-3}].

the irreversible character of the matrix dissolution is demonstrated. The macroscopic conductivity during chemical un- and reloading follows the same curve as non-reactive porous materials for $c \geqslant \kappa_c$ (compare Fig. 2). It is determined by the porosity related to the current state of chemical degradation $\phi(\kappa_c)$ ($\kappa_c = 0.8c_0$ or $\kappa_c = 0.4c_0$) and Kohlrausch's law. If the current calcium concentration c in the pore fluid reaches again values smaller than the current threshold κ_c, the system again changes to a reactive porous material (compare Fig. 5), characterized by matrix dissolution, changing porosity and a conductivity which is controlled by the concentration, the porosity and the matrix dissolution. As expected, higher levels of mechanical degradation are connected with a higher conductivity. In the stress–strain relations on the right-hand side of Fig. 7 the reduction of stiffness and strength due to coupled chemo-mechanical damage ($\kappa_c/c_0 < 1$) can be observed.

3.7. Dimensional analysis of Ca^{2+} storage/source terms

Since the storage term $[[\phi_0 + \phi_c]c]^{\cdot}$ of the calcium mass balance (Eq. (9)) connected to the change of the pore space and the concentration within the interstitial pore solution is neglected in most of the existing chemo-mechanical damage models (see e.g. Delagrave et al., 1997; Gérard, 1996, 2000; Mainguy et al., 2000; Torrenti et al., 1998; Ulm et al., 1999), a dimensional analysis of the storage term $[[\phi_0 + \phi_c]c]^{\cdot}$ and the source term $\dot{s}$ is performed in order to estimate its relevance for the modeling of calcium dissolution–diffusion processes. The storage term is additively decomposed into the terms $\dot{c}_{\phi 1}$ and $\dot{c}_{\phi 2}$ associated with the change of the chemically induced porosity and the change of the calcium concentration of the pore fluid:

$$\dot{c}_\phi = \dot{c}_{\phi 1} + \dot{c}_{\phi 2} = \dot{\phi}_c c + [\phi_0 + \phi_c]\dot{c}, \qquad \dot{\phi}_c = \frac{\partial \phi_c}{\partial s}\dot{s} = \frac{\partial \phi_c}{\partial s}\frac{\partial s}{\partial \kappa_c}\frac{\partial \kappa_c}{\partial c}\dot{c} \qquad (39)$$

For chemical loading processes (otherwise $\dot{s}$ is zero and the dimensional analysis is not meaningful) $\partial \kappa_c/\partial c = 1$. The derivatives $\partial \phi_c/\partial s = \mathcal{M}/\rho$ and $\partial s/\partial \kappa_c$ are given by Eq. (A.2). From Eq. (39), the ratios of the terms $\dot{c}_\phi$ and $\dot{s}$ can be calculated:

$$\frac{\dot{c}_\phi}{\dot{s}} = \frac{\dot{c}_{\phi 1}}{\dot{s}} + \frac{\dot{c}_{\phi 2}}{\dot{s}} = \frac{\partial \phi_c}{\partial s}c + \frac{\phi_0 + \phi_c}{\partial s/\partial \kappa_c} \qquad (40)$$

For the dimensional analysis, the conditions of dissociating portlandite (p), ettringite (e) and CSH-phases (csh) are considered separately. Consequently, Eq. (40) is evaluated for the related equilibrium concentrations:

$$\left[\frac{\dot{c}_{\phi 1}}{\dot{s}}\right]_{\mathrm{p}} = -\frac{\mathcal{M}}{\rho}c_{\mathrm{p}} = -6.65 \times 10^{-4}, \qquad \left[\frac{\dot{c}_{\phi 2}}{\dot{s}}\right]_{\mathrm{p}} = \frac{\phi_0 + \phi_c(c_{\mathrm{p}})}{\partial s(c_{\mathrm{p}})/\partial \kappa_c} = 4.53 \times 10^{-5}$$

$$\left[\frac{\dot{c}_{\phi 1}}{\dot{s}}\right]_{\mathrm{e}} = -\frac{\mathcal{M}}{\rho}c_{\mathrm{e}} = -3.50 \times 10^{-4}, \qquad \left[\frac{\dot{c}_{\phi 2}}{\dot{s}}\right]_{\mathrm{e}} = \frac{\phi_0 + \phi_c(c_{\mathrm{e}})}{\partial s(c_{\mathrm{e}})/\partial \kappa_c} = 2.27 \times 10^{-3} \qquad (41)$$

$$\left[\frac{\dot{c}_{\phi 1}}{\dot{s}}\right]_{\mathrm{csh}} = -\frac{\mathcal{M}}{\rho}c_{\mathrm{csh}} = -5.25 \times 10^{-5}, \qquad \left[\frac{\dot{c}_{\phi 2}}{\dot{s}}\right]_{\mathrm{csh}} = \frac{\phi_0 + \phi_c(c_{\mathrm{csh}})}{\partial s(c_{\mathrm{csh}})/\partial \kappa_c} = 1.34 \times 10^{-4}$$

ϕ_c and $\partial s/\partial \kappa_c$ are calculated for equilibrium concentrations corresponding to the dissolution of portlandite, ettringite and CSH by means of Eqs. (19), (20) and (A.2). The average equilibrium concentration of ettringite is estimated as $c_{\mathrm{e}} \approx 10$ mol/m³. In Fig. 8 the storage terms $\dot{c}_{\phi 1}$, $\dot{c}_{\phi 2}$ and $\dot{c}_\phi$ are compared to the dissolution rate $\dot{s}$ for chemical loading ($c = \kappa_c$) within the range $c \in [0, c_0]$. The maximum value of the ratio $\dot{c}_\phi/\dot{s}$ is approximately 10^{-2}. In the case of portlandite and CSH dissolution $\dot{s}$ is approximately 10^3–10^4 times
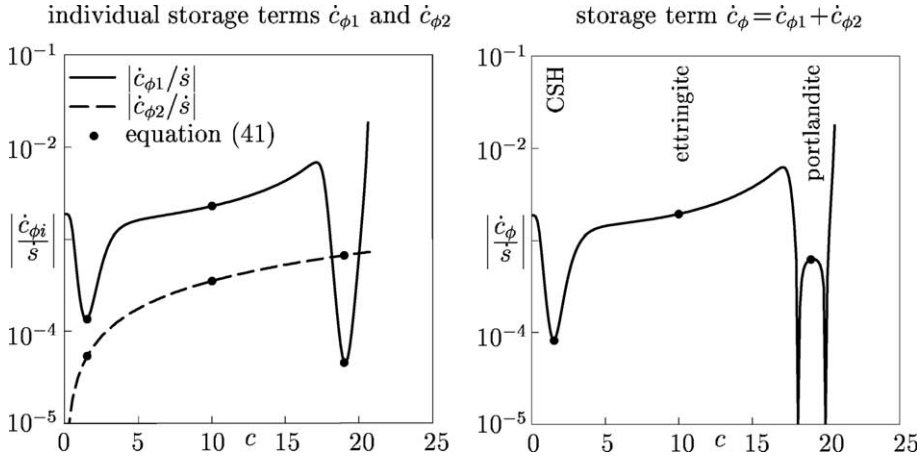
Fig. 8. Dimensional analysis of Ca^{2+} storage/source terms $\dot{c}_{\phi 1}/\dot{s}$, $\dot{c}_{\phi 2}/\dot{s}$ and $\dot{c}_{\phi}/\dot{s}$ for monotonic chemical loading ($c = \kappa_c$).

larger compared to the terms $\dot{c}_{\phi 1}$, $\dot{c}_{\phi 2}$ and $\dot{c}_{\phi}$. Hence, it is concluded, that the term $\dot{c}_{\phi}$ can be neglected for chemical loading. However, in the chemical unloading regime ($\dot{s} = 0$), this term controls the transient behavior of the diffusion according to the calcium ion mass balance (9). Furthermore, from the differences between the terms $\dot{s}$ and $\dot{c}_{\phi}$ it can be expected, that the time scales of dissociation-diffusion (chemical loading) and diffusion (chemical unloading) processes are significantly different.

4. Conclusions

A material model describing the deterioration of cementitious materials such as concrete resulting from coupled calcium leaching and micro-cracking is developed in the present paper. The model is based on the description of concrete as a porous medium composed by the connected fluid filled pore space and the cementitious skeleton. The volume fraction of the pores controls the macroscopic material properties such as stiffness, strength and conductivity. The pore space can be subdivided in three types of porosity: The initial porosity, the porosity induced by the dissolution of the cementitious substances due to dissociation and the apparent pore space related to the opening of micro-cracks and micro-pores within the skeleton. Matrix dissolution and mechanical damage of the skeleton are described in an equivalent manner by the definition of history variables and phenomenological models characterizing the irreversible state and progress of degradation of both dissipative processes. The thermodynamic framework of the model allows for the consistent derivation of loading/unloading criteria for chemical dissolution as well as for mechanical damage. Based on the assumptions of chemical and mechanical potentials macroscopic constitutive laws are consistently formulated within the theory of mixtures. With this approach further empirical models or assumptions are circumvented. Extensive model studies illustrate the main characteristic of the present chemo-mechanical damage model with regards to modeling of ion transport and chemo-mechanical couplings. Its ability to capture non-linear conductivity caused by ion–ion interactions, the reduction of stiffness and strength and the increasing conductivity corresponding to chemically and mechanically induced damage are demonstrated. The presentation of the proposed model will be supplemented by the second part of the paper by Kuhl et al. (in press). This part is concerned with the development of numerical methods for coupled chemo-mechanical analyses and their application to durability oriented simulations of concrete structures.

Acknowledgements

Appendix A. Consistent linearization of constitutive laws

This appendix provides derivatives required for the linearization of the constitutive laws of the chemo-mechanical model developed in this paper. The consistent linearization of the mass flux vector $\boldsymbol{q}$ (31) and the stress tensor $\boldsymbol{\sigma}$ (31) contain the following terms using the definition $\Delta\gamma = \partial\gamma/\partial c\,\Delta c$:

$$
\begin{aligned}
\frac{\partial \boldsymbol{q}}{\partial c}\Delta c &= \left[[1-d_m]\frac{\partial \phi_c}{\partial s}\frac{\partial s}{\partial \kappa_c}\frac{\partial \kappa_c}{\partial c}\boldsymbol{D}_0 \cdot \gamma + \phi\frac{\partial \boldsymbol{D}_0}{\partial c} \cdot \gamma\right]\Delta c + \phi\boldsymbol{D}_0 \cdot \Delta\gamma \\
\frac{\partial \boldsymbol{q}}{\partial \boldsymbol{\varepsilon}}:\Delta\boldsymbol{\varepsilon} &= \left[[1-\phi_0-\phi_c]\frac{\partial d_m}{\partial \kappa_m}\frac{\partial \kappa_m}{\partial \eta}[\boldsymbol{D}_0 \cdot \gamma]\otimes\frac{\partial \eta}{\partial \boldsymbol{\varepsilon}}\right]:\Delta\boldsymbol{\varepsilon} \\
\frac{\partial \boldsymbol{\sigma}}{\partial c}\Delta c &= [d_m-1]\mathscr{C}_0 : \boldsymbol{\varepsilon}\frac{\partial \phi_c}{\partial s}\frac{\partial s}{\partial \kappa_c}\frac{\partial \kappa_c}{\partial c}\Delta c \\
\frac{\partial \boldsymbol{\sigma}}{\partial \boldsymbol{\varepsilon}}:\Delta\boldsymbol{\varepsilon} &= \left[[1-\phi]\mathscr{C}_0 - [1-\phi_0-\phi_c][\mathscr{C}_0 : \boldsymbol{\varepsilon}]\otimes\frac{\partial d_m}{\partial \kappa_m}\frac{\partial \kappa_m}{\partial \eta}\frac{\partial \eta}{\partial \boldsymbol{\varepsilon}}\right]:\Delta\boldsymbol{\varepsilon}
\end{aligned}
\tag{A.1}
$$

Herein, the first derivative of the concentration s (Eq. (19), for $0 < c < c_0$) with respect to the internal variable κ_c, the derivative of the chemically induced porosity ϕ_c (20) with respect to the calcium concentration of the skeleton s and the derivative of the conductivity tensor $\boldsymbol{D}_0$ (13) with respect to the concentration have to be calculated. Furthermore, the second derivative of $s(\kappa_c)$ is provided for the numerical solution of coupled chemo-mechanical initial boundary value problems, addressed in the second part of the present paper (Kuhl et al., in press):

$$
\begin{aligned}
\frac{\partial s}{\partial \kappa_c} &= [1-\alpha_c]s_\mathrm{h}\left[\frac{1}{10\bar{c}} - \frac{\kappa_c}{200\bar{c}^2}\right] + \frac{n[s_0-s_\mathrm{h}]\kappa_c^{n-1}}{c_\mathrm{p}^n\left[1+\left[\frac{\kappa_c}{c_\mathrm{p}}\right]^n\right]^2} + \frac{m\alpha_c s_\mathrm{h}\kappa_c^{m-1}}{c_\mathrm{csh}^m\left[1+\left[\frac{\kappa_c}{c_\mathrm{csh}}\right]^m\right]^2} \\
\frac{\partial^2 s}{\partial \kappa_c^2} &= \frac{[\alpha_c-1]s_\mathrm{h}}{200\bar{c}} + \frac{n[n-1][s_0-s_\mathrm{h}]\kappa_c^{n-2}}{c_\mathrm{p}^n\left[1+\left[\frac{\kappa_c}{c_\mathrm{p}}\right]^n\right]^2} - \frac{2n^2[s_0-s_\mathrm{h}]\kappa_c^{2n-2}}{c_\mathrm{p}^{2n}\left[1+\left[\frac{\kappa_c}{c_\mathrm{p}}\right]^n\right]^3} \\
&\quad + \frac{m[m-1]\alpha_c s_\mathrm{h}\kappa_c^{m-2}}{c_\mathrm{csh}^m\left[1+\left[\frac{\kappa_c}{c_\mathrm{csh}}\right]^m\right]^2} - \frac{2m^2\alpha_c s_\mathrm{h}\kappa_c^{2m-2}}{c_\mathrm{csh}^{2m}\left[1+\left[\frac{\kappa_c}{c_\mathrm{csh}}\right]^m\right]^3} \\
\frac{\partial \phi_c}{\partial s} &= -\frac{\mathscr{M}}{\rho} \\
\frac{\partial \boldsymbol{D}_0}{\partial c} &= -\frac{D_{0c}}{2\sqrt{c}}\mathbf{1}
\end{aligned}
\tag{A.2}
$$

As far as the mechanical elasto-damage model is concerned, the linearizations of the equivalent strain η (29) with respect to the strain tensor $\boldsymbol{\varepsilon}$ and the scalar damage parameter d_m (30) with respect to the internal parameter κ_m are given below:

$$\frac{\partial \eta}{\partial \boldsymbol{\varepsilon}} = \frac{1}{E_0 \eta} \mathscr{C}_0 : \boldsymbol{\varepsilon}$$

$$\frac{\partial d_m}{\partial \kappa_m} = \frac{\kappa_m^0}{\kappa_m^2} \left[1 - \alpha_m + \alpha_m [1 + \beta_m \kappa_m] \exp[\beta_m[\kappa_m^0 - \kappa_m]] \right] \tag{A.3}$$

References

Adenot, F., 1992. Durabilité du béton: Caractérisation et modélisation des processus physiques et chimiques de dégradation du ciment. Ph.D. Thesis, Université d'Orléans.

Adenot, F., Buil, M., 1992. Modelling of the corrosion of the cement paste by deionized water. Cement and Concrete Research 22, 489–496.

Arroyo, M., Díez, P., Huerta, A., 2000. Coupled chemo-mechanical computations of concrete degradation: control of accuracy. Technical Report, Department de Mathemàtica Aplicada III, Universitat Politècnica de Catalunya, Barcelona.

Atkins, P., 1998. Physical Chemistry. Oxford University Press, Oxford.

Bangert, F., Kuhl, D., Meschke, G., 2001. Finite element simulation of chemo-mechanical damage under cyclic loading conditions. In: de Borst, R., Mazar, J., Pijaudier-Cabot, G., van Mier, J. (Eds.), Fracture Mechanics of Concrete Structures. Balkema Publishers, Lisse, pp. 207–214.

Berner, U., 1988. Modelling the incongruent dissolution of hydrated cement minerals. Radiochimica Acta 44–45, 387–393.

Berner, U., 1992. Evolution of pore water chemistry during degradation of cement in a radioactive waste repository environment. Waste Management 12, 201–219.

Bowen, R., 1976. Theory of mixtures. In: Eringen, A. (Ed.), Continuum Physics. Academic Press, New York, pp. 1–127.

Carde, C., François, R., 1997. Effect on the leaching of calcium hydroxide from cement paste on mechanical properties. Cement and Concrete Research 27, 539–550.

Carde, C., François, R., Torrenti, J.-M., 1996. Leaching of both calcium hydroxide and C–S–H from cement paste: modelling the mechanical behavior. Cement and Concrete Research 22, 1257–1268.

Carde, C., Escadeillas, G., François, R., 1997a. Use of ammonium nitrate solution to simulate and accelerate the leaching of cemente pastes due to deionized water. Magazine of Concrete Research 49, 295–301.

Carde, C., François, R., Ollivier, J.-P., 1997b. Microstructural changes and mechanical effects due to the leaching of calcium hydroxide from cement paste. In: Scrivener, K., Young, J. (Eds.), Mechanics of Chemical Degradation of Cement-Based Systems. Chapman & Hall, London, pp. 30–37.

Coussy, O., 1995. Mechanics of Porous Continua. John Wiley & Sons, Chicester.

Coussy, O., Ulm, F.-J., 2001. Elements of durability mechanics of concrete structures. In: Ulm, F.-J., Bažant, Z., Wittmann, F. (Eds.), Creep, Shrinkage and Durability Mechanics of Concrete and other Quasi-Brittle Materials. Elsevier Science, Amsterdam, pp. 3993–4009.

Coussy, O., Ulm, F.-J., Mainguy, M., 1999. A Short-course on Environmental Mechanics of Concrete, International Centre for Mechanical Sciences, cISM Courses and Lectures Springer-Verlag, Berlin.

de Vree, J., Brekelmans, W., van Gils, M., 1996. Comparison of nonlocal approaches in continuum damage mechanics. Computers & Structures 55, 581–588.

Debye, P., Hückel, E., 1923. Zur Theorie der Elektrolyte. II. Grenzgesetz für die elektrische Leitfähigkeit. Physikalische Zeitschrift 24 (15), 305–325.

Delagrave, A., Gérard, B., Marchand, J., 1997. Modelling the calcium leaching mechanisms in hydrated cement pastes. In: Scrivener, K., Young, J. (Eds.), Mechanics of Chemical Degradation of Cement-Based Systems. Chapman & Hall, London, pp. 30–37.

Díez, P., Arroyo, M., Huerta, A., 2002. Adaptive simulation of the coupled chemo-mechanical concrete degradation. In: Mang, H., Rammerstorfer, F., Eberhardsteiner, J. (Eds.), Proceedings of the Fifth World Congress on Computational Mechanics, WCCM V, Vienna University of Technology, Vienna.

Fick, A., 1855. Ueber Diffusion. Annalen der Physik und Chemie 94 (1), 59–86.

Gérard, B., 1996. Contribution des couplages mécanique-chimie-transfert dans la tenue a long terme des ouvrages de stockage de déchets radioactifs. Ph.D. Thesis, Laboratoire de Méchanique et Technologie, E.N.S. de Cachan.

Gérard, B., 2000. Hydrolysis of cement-based materials: a review. In: Setzer, M. (Ed.), Pore Solution in Hardened Cement Paste. Aedificatio Publishers, Freiburg, pp. 271–304.

Gérard, B., Pijaudier-Cabot, G., La Borderie, C., 1998. Coupled diffusion-damage modelling and the implications on failure due to strain localisation. International Journal of Solids and Structures 35, 4107–4120.

Heukamp, F., Ulm, F.-J., Germaine, J., 2001a. Mechanical properties of calcium leached cement paste: triaxial stress states and the influence of pore pressure. Cement and Concrete Research 31, 767–774.

Heukamp, F., Mainguy, M., Ulm, F.-J., 2001b. Beyond the crack size criterion: the effect of a fracture on calcium leaching depletion of cementious materials. In: de Borst, R., Mazar, J., Pijaudier-Cabot, G., van Mier, J. (Eds.), Fracture Mechanics of Concrete Structures. Balkema Publishers, Lisse, pp. 215–221.

Jirásek, M., Bažant, Z., 2002. Inelastic Analysis of Structures. John Wiley & Sons, Chichester.

Kachanov, L., 1958. Time rupture process under creep conditions. Izvestija Akademii Nauk Sojuza Sovetskich Socialisticeskich Respubliki (SSSR) Otdelenie Techniceskich Nauk (Moskra) 8, 26–31.

Kohlrausch, F., 1900. Über das elektrische Leitvermögen von Lösungen der Alkali-Jodate und eine Formel zur Berechnung von Leitvermögen. Sitzungsberichte der königlich preussischen Akademie für Wissenschaften, pp. 1002–1008.

Kohlrausch, F., von Steinwehr, H., 1902. Weitere Untersuchungen über das Leitvermögen von Elektrolyten aus einwertigen Ionen in wässriger Lösung. Sitzungsberichte der königlich preussischen Akademie für Wissenschaften, pp. 581–587.

Krajcinovic, D., 1996. Damage Mechanics. Elsevier Science, Amsterdam.

Kuhl, D., Bangert, F., Meschke, G., 2000. An extension of damage theory to coupled chemo-mechanical processes. In: Oñate, E. (Ed.), European Congress on Computational Methods in Applied Science and Engineering, Barcelona.

Kuhl, D., Bangert, F., Meschke, G., in press. Coupled chemo-mechanical deterioration of cementitious materials. Part II: Numerical methods and simulations. International Journal of Solids and Structures, in this issue.

Le Bellégo, C., Gérard, B., Pijaudier-Cabot, G., 2000. Chemo-mechanical effects in motar beams subjected to water hydrolysis. Journal of Engineering Mechanics 126, 266–272.

Le Bellégo, C., Gérard, B., Pijaudier-Cabot, G., 2001a. Mechanical analysis of concrete structures submitted to aggressive water attack. In: de Borst, R., Mazar, J., Pijaudier-Cabot, G., van Mier, J. (Eds.), Fracture Mechanics of Concrete Structures. Balkema Publishers, Lisse, pp. 239–246.

Le Bellégo, C., Gérard, B., Pijaudier-Cabot, G., 2001b. Life-time experiments on mortar beams submitted to calcium leaching. In: Ulm, F.-J., Bažant, Z., Wittmann, F. (Eds.), Creep, Shrinkage and Durability Mechanics of Concrete and Other Quasi-Brittle Materials. Elsevier Science, Amsterdam, pp. 493–498.

Le Bellégo, C., Gérard, B., Pijaudier-Cabot, G., Dubé, J.-F., Molez, L., 2003. Coupled mechanical and chemical damage in calcium leached cementitious structures. Journal of Engineering Mechanics 129 (3), 333–341.

Lemaître, J., 1996. A Course on Damage Mechanics. Springer-Verlag, Berlin.

Lemaître, J., Chaboche, J., 1990. Mechanics of Materials. Cambridge University Press, Cambridge.

Mainguy, M., 1999. Modellés de diffusion non-linéaires en milieux poreux. Applications á la dissolution et au séchage des matériaux cimentaires. Ph.D. Thesis, L'Ecole Nationale Des Ponts et Chaussés.

Mainguy, M., Coussy, O., 2000. Propagation fronts during calcium leaching and cloride penetration. Journal of Engineering Mechanics 126, 250–257.

Mainguy, M., Ulm, F.-J., 2000. Coupled diffusion-dissolution around a fracture channel: the solute congestion phenomenon. International Journal for Transport in Porous Media 6, 1–19.

Mainguy, M., Tognazzi, C., Torrenti, J.-M., Adenot, F., 2000. Modelling of leaching in pure cement paste and motar. Cement and Concrete Research 30, 83–90.

Mainguy, M., Ulm, F.-J., Heukamp, F., 2001. Similarity properties of demineralization and degradation of cracked porous materials. International Journal of Solids and Structures 38, 7079–7100.

Mazars, J., 1986. A description of micro- and macroscale damage of concrete structures. International Engineering Fracture Mechanics 25, 729–737.

Onsager, L., 1927. Report on a revision of the conductivity theory. In: Desche, C. (Ed.), The Theory of Strong Electrolytes. A General Discussion. In: Transactions of the Faraday Society, vol. 23, pp. 341–356.

Pijaudier-Cabot, G., Gérard, B., Molez, L., 1998a. Damage mechanics of concrete structures subjected to mechanical and environmental actions. In: de Borst, R., Bićanić, N., Mang, H., Meschke, G. (Eds.), Computational Modelling of Concrete Structures. Balkema, Rotterdam, pp. 559–566.

Pijaudier-Cabot, G., Gérard, B., Burlion, N., Molez, L., 1998b. Localisation of damage in quasi-brittle materials and influence of chemically activated damage. In: de Borst, R., van der Giessen, E. (Eds.), Material Instabilities in Solids. John Wiley & Sons, Chicester, pp. 441–456.

Pijaudier-Cabot, G., Haidar, K., Omar, M., 2002. Non local damage approaches in durability mechanics: influence of the length scale in coupled problems. In: Mang, H., Rammerstorfer, F., Eberhardsteiner, J. (Eds.), Proceedings of the Fifth World Congress on Computational Mechanics, WCCM V, Vienna University of Technology, Vienna.

Simo, J., Hughes, T., 1998. Computational Inelasticity. Springer-Verlag, New York.

Simo, J., Ju, J., 1987. Strain- and stress-based continuum damage models. International Journal of Solids and Structures 23, 821–869.

Taylor, H., 1997. Cement Chemistry. Thomas Telford, London.

Torrenti, J.-M., Mainguy, M., Adenot, F., Tognazzi, C., 1998. Modelling of leaching in concrete. In: de Borst, R., Bićanić, N., Mang, H., Meschke, G. (Eds.), Computational Modelling of Concrete Structures. Balkema, Rotterdam, pp. 559–566.

Trägårdh, J., Lagerblad, B., 1998. Leaching of 90-year old concrete mortar in contact with stagnant water. Technical Report, TR-98-11, Swedish Cement and Concrete Research Institute, Stockholm.

Ulm, F.-J., Torrenti, J.-M., Adenot, F., 1999. Chemoporoplasticity of calcium leaching in concrete. Journal of Engineering Mechanics 125, 1200–1211.

Ulm, F.-J., Heukamp, F., Germaine, J., 2001. Durability mechanics of calcium leaching of concrete and beyond. In: de Borst, R., Mazar, J., Pijaudier-Cabot, G., van Mier, J. (Eds.), Fracture Mechanics of Concrete Structures. Balkema Publishers, Lisse, pp. 133–143.